BIOACTIVE PEPTIDE NANOFIBERS FOR ACCELERATION OF BURN WOUND HEALING

A THESIS SUBMITTED TO

THE GRADUATE SCHOOL OF ENGINEERING AND SCIENCE

OF BILKENT UNIVERSITY

IN PARTIAL FULFILLMENT OF THE REQUIREMENTS FOR

THE DEGREE OF

MASTER OF SCIENCE

IN

MATERIALS SCIENCE AND NANOTECHNOLOGY

By

FATİH YERGÖZ

May, 2017

BIOACTIVE PEPTIDE NANOFIBERS FOR ACCELERATION OF BURN WOUND HEALING

By Fatih Yergöz,

May, 2017

We certify that we have read this thesis and that in our opinion it is fully adequate, in scope and in quality, as a dissertation for the degree of Master of Science.

Ayşe Begüm Tekinay (Advisor)

Aykutlu Dâna

Reyhan Neslihan Gürsoy

Approved for the Graduate School of Engineering and Science:

Ezhan Karaşan

Director of the Graduate School

ABSTRACT

BIOACTIVE PEPTIDE NANOFIBERS FOR ACCELERATION OF BURN WOUND HEALING

Fatih Yergöz

M.Sc. in Materials Science and Nanotechnology

Supervisor: Ayşe Begüm Tekinay

May, 2017

Burn injuries are one of the most typical types of trauma worldwide, and the unique physiology of burn injuries requires the use of specialized therapeutic materials for treatment and makes the development of such materials especially challenging. Here, we report the use of synthetic, functional and biodegradable peptide nanofiber gels for improved healing of burn wounds to alleviate the progressive loss of tissue function at the post-burn wound site. These bioactive nanofiber gels form scaffolds which recapitulate the morphology and function of the natural extracellular matrix through peptide epitopes, which can trigger angiogenesis through significant affinity to basic growth factors. In this study, the angiogenesis-promoting properties of the bioactive scaffolds were utilized for the treatment of thermal burn model. Following the excision of necrotic tissue, bioactive gels and control solutions were applied topically onto the wound area. The wound healing process was evaluated at 7, 14 and 21 days following injury through histological observations, immunostaining and marker RNA / protein analysis. Bioactive peptide nanofiber treated burn wounds formed well-organized and collagen-rich granulation tissue layers, developed a greater density of

newly formed blood vessels, and exhibited increased re-epithelialization and skin appendage formation with minimal crust formation. Overall, the heparin-mimetic peptide nanofiber gels increased the rate of repair of burn injuries and can be used as effective means of facilitating wound healing.

Keywords: Peptide Nanofiber, Burn Injury, Heparin, Hydrogel, Self-Assembly, Neo-vascularization, Extracellular matrix

ÖZET

YANIK YARA İYİLEŞMESİNİN HIZLANDIRILMASINDA BİYOAKTİF PEPTİT NANOFİBERLERİN KULLANIMI

Fatih Yergöz

Malzeme Bilimi ve Nanoteknoloji, Yüksek Lisans

Danışman: Ayşe Begüm Tekinay

May, 2017

Yanık yaralanmaları dünya genelinde en yaygın travma tiplerinden biri olmakla birlikte yanık yaralanmalarının kendine özgü fizyolojisi, tedavi için özel terapötik materyallerin kullanılmasını gerektirmekte ve bu tür malzemelerin geliştirilmesini zorlaştırmaktadır. Bu tez kapsamında, yanık yaralanmaları sonucu yara alanında oluşan ilerleyici doku fonksiyonu kaybının hafifletilerek iyileştirilmesi için sentetik, fonksiyonel ve biyolojik olarak parçalanabilir peptit nanofiber jellerin kullanımı anlatılmaktadır. Bu biyoaktif nanofiber jelleri bazik büyüme faktörlerine kuvvetli afiniteyle bağlanarak anjiyogenezi tetikleyebildigi gibi, hücrelere sinyal verebilen peptit epitopları vasıtasıyla hücreler arası ortamın yapısını ve fonksiyonunu taklit edebilme yetisine sahip iskeleler oluşturabilmektedir. Bu çalışmada, biyoaktif iskelelerin anjiyogenezi teşvik edici özellikleri termal yanık yara modelinin tedavisinde kullanılmıştır. Nekrotik dokuların eksizyonunu takiben, biyoaktif jel ve kontrol solusyonları yara alanı üzerine topikal olarak uygulanmıştır. Yaranın iyileşme süreci hasar sonrası 7., 14. ve 21. günlerde histolojik gözlemler, immüno boyama ve markör RNA / protein analizi ile değerlendirilmiştir. Biyoaktif peptit nanofiber ile

tedavi edilen yanık yaralarında, iyi organize olmuş ve kollajen bakımından zengin granülasyon dokusu, yara alanında yeni oluşan kan damarlarının yoğunluğunda, minimal kabuk oluşumu ile yeni oluşturulan epitelizasyon ve deri apendiksiyonu seviyesinde artma gözlemlenmiştir. Sonuç olarak, heparin-mimetik peptit nanofiber jelleri yanık yaralanmalarının onarımını arttırmasıyla, yara iyileşmesini kolaylaştırmada etkili bir tedavi yöntemi olarak kullanılabilir.

Anahtar sözcükler: Peptit Nanofiber, Yanık Yarası, Heparin, Hidrojel, Kendindiliğinden Bir Araya Gelme, Neo-vaskülarizasyon, Ekstraselüler matris

ACKNOWLEDGEMENT

There are numerous people to acknowledge for their cooperation, guidance and support during the last two years. So many have made my stay in Ankara a lot easier that I thought it was going to be. This thesis would not have been possible without the help and support of the kind people around me, to only some of whom it is possible to give particular mention here.

It would not have been possible to write this master thesis without continuous motivation and patience of my primary advisor Prof. Ayşe Begüm Tekinay. I appreciate her vast knowledge and skill in many areas not to mention her guidance, advice, and constant, horrifying academic pressure that were responsible for the completion of my thesis in a timely manner, and resulted in the preparation of a high-quality manuscript in the process. The door of Prof. Tekinay office was always open and she was always interested whenever I had a question about my research and writing or encountered trouble related with my experiments. It was a great opportunity to be advised by someone communicative, diligent, enthusiastic and friendly for my master study.

I would like to thank my thesis committee, Dr. Dâna and Dr. Gürsoy for the assistance they provided to make this thesis with high-standards by improving it from various perspectives and for taking time out from their busy schedule to serve as my external reader. I would also like to thank Dr. Mustafa Özgür Güler, who was gracious enough to read and comment on much of my work and gave access to his laboratory and research facilities.

With a special mention, I am thankful to my lifetime friends from IYTE, Nurcan Hastar, İdil Uyan, Merve Şen, Zeynep Orhan, Gökhan Günay for the stimulating

discussions, for the sleepless nights we were working together, and for all the fun we have had in the two years. It was fantastic to have the opportunity to work majority of my master research beside you!

I would like to thank all NBT, BML and other UNAM members especially Cağla Eren, Begüm Dikeçoğlu, Faruk Okur, Mustafa Fadlelmula, Özge Uysal, Sehmus Tohumeken, Burak Demircan, İslam Oğuz Tuncay, Canelif Yılmaz, İbrahim Çelik, Mustafa Beter, Abdurrahman Türksoy and Deniz Yıldız for creating such a warm and entertaining working environment.

The assistance, cooperation and experience of my fellow doctoral students and pos-doc's were essential for the completion of the field as well as the model deck. I'd like to thank Gülistan Tansık, Elif Arslan, Nuray Gündüz, Melike Sever, Özlem Tufanlı, Dr. Begüm Kocatürk, Dr. Muhammed Aref Khaliy, Ahmet Emin Topal. In particular, I am grateful to Dr. Gözde Uzunallı for enlightening me the first glance of research.

I would also like to thank Alper Devrim Özkan as the first reader and reviewer of this thesis, and I am very grateful to him for his very valuable comments and revision on this thesis.

My forever interested, encouraging and always enthusiastic grandmother Ülker Tozlu and grandfather Sabri Yergöz: they were always keen to know what I was doing, although it is likely that they never grasped what it was all about! I will miss your screams of joy whenever a significant momentous was reached.

I would like to acknowledge the financial and technical support of National Nanotechnology Research Center (UNAM). Much of the experimental work would

not have been completed without the equipment and technical assistance of technicians.

I would like to acknowledge the financial assistance of The Scientific and Technological Research Council of Turkey (TÜBİTAK) under the BİDEB 2210/C Master Scholarship.

Finally, I would like to express my very profound appreciation to my father Mehmet Emin & my mother Neslihan and my brothers Enes & Arif Emre and to my girlfriend Nurcan for providing me with unfailing support, for their continuous encouragement, personal support, great patience and endless love throughout my master studies and through the process of researching and writing this thesis. These accomplishments wouldn’t have been possible without them. Thank you.

Fatih

Table of Contents

Abbreviations

AFM	Atomic force microscopy
ANOVA	Analysis of variance
Boc	*Tert*-butoxycarbonyl
BSA	Bovine serum albumin
CD	Circular dichroism
CS	Chondroitin sulfate
Col-I	Collagen type I
DAB	3,3'-diaminobenzidine
DCM	Dichloromethane
DMEM	Dulbecco's modified Eagle's medium
DMF	N,N-Dimethylformamide
DMSO	Dimethyl sulfoxide
ECM	Extracellular matrix
EDTA	Ethylenediaminetetraacetic acid
E-PA	Lauryl-VVAGE-OH
ESC	Embryonic stem cells
FBS	Fetal bovine serum
FDA	U.S. Food and Drug Administration
FGF-2	Fibroblast growth factor-2
Fmoc	9-Fluorenylmethoxycarbonyl
GAG	Glycosaminoglycan
GF	Growth factor

H&E	Hematoxylin and eosin
HBTU	*N*,*N*,*N*′,*N*′-Tetramethyl-O-(1*H*-benzotriazole-1-yl) uronium hexafluorophosphate
HM-PA	Heparin mimetic peptide amphiphile
HPLC	High pressure liquid chromatography
HRP	Horseradish peroxidase
HKT	Human keratocyte
HUVEC	Human umbilical vein endothelial cell
IHC	Immunohistochemistry
IPGTT	Intraperitoneal glucose tolerance test
iPSC	Induced pluripotent stem cell
K-PA	Lauryl-VVAGK- NH_2
LC-MS	Liquid chromatography-Mass spectroscopy
P/S	Penicillin/Streptomycin
PA	Peptide amphiphile
PBS	Phosphate buffered saline
PDGF	Platelet-derived growth factor
PEG	Poly ethylene glycol
RT	Room temperature
SEM	Standard error of mean
SDS	Sodium dodecyl sulfate
T1D	Type 1 Diabetes
TBS	Tris buffered saline
TCP	Tissue culture plate
TEM	Transmission electron microscopy

TIS	Triisopropylsilane
TFA	Trifluoroacetic acid

List of Figures

List of Tables

CHAPTER 1

INTRODUCTION

1.1. Skin and Burns - Overview

Although skin is the largest organ of the body, it is also least appreciated. It serves as a protective barrier by covering external surface of the human body and prevents internal tissues from being exposed to trauma, radiation, dehydration, and infection. It also helps thermoregulation process of the body through the action of hair follicles, sweating, vasoconstriction, and vasodilation. The skin gathers sensory information from the surrounding environment, assists in vitamin D synthesis as well as plays a crucial roles in the activation of the immune system against external pathogens. However, skin is almost wholly exposed to the external world and therefore is susceptible to constant wear and damage. While minor abrasions can be repaired with ease, severe skin injuries require medical intervention to prevent infection and fluid loss during the "down period" in which the skin tissue is non-functional. Amongst skin injuries requiring medical attention, burn wounds are some of the most common.

Burns can be caused by sources of thermal, chemical and electrical energy, as well as radiation. The most common type of burn injury is thermal burns which are classified into three groups depending on their severity.

1. Only the outermost layer (epidermis) of the skin is damaged in first degree burns, do not necessitate medical attention, and heal rapidly. The nervous system underneath the skin is intact in these burns, resulting in considerable pain.
2. Epidermis and the layer beneath it (dermis) is damaged in second degree burns.
3. Complete destruction of skin tissues to its full depth (epidermis, dermis and subcutaneous layers) is observed in third degree burns, and severe damage to

underlying tissues including fat, muscles and nerves. As a consequence of the latter, they are predominantly painless.

1.1.1. Socio-Economic Impact

There are around 2,000,000 burn injury cases that require medical attention in United States each year, of which 70,000 require hospitalization and 20,000 are treated in specialized burn centers. Burn wounds create a breach in the defense mechanisms of the body, making patients vulnerable to secondary infections by viruses and bacteria. These infections are responsible for about 10,000 deaths each year. Due to the risk of infection, victims of severe burn injuries must be treated in intensive care units and incur very high costs as a consequence.

1.1.2. Etiology of burn wounds

Although, there are several sources of burn wounds, their treatment is generally similar regardless of their origin since destruction of tissue is observed in all of the burns. Thermal burns will be discussed in the scope of this thesis. Severity of burns is determined mainly by two factors; the temperature, and the exposure time. Burns can occur at surprisingly low temperatures; permenant damage is observed at temperature as low as 44 ^{o}C in human skin according to previous experiments. The natural repair mechanism of skin cells cannot handle damage accumulation rate above this temperatures. While cells can nevertheless endure heat above this threshold for a considerable time, time before tissue necrosis decreases substantially if temperature is raised further above it. Since the severity of damage increases with temperature, sufficiently high temperatures can result in the destruction of all layers of tissue structure, including the extracellular matrix. The fluid flow to the site of injury is also impaired in burn wounds, limiting the transportation of oxygen and nutrients to the wound site, and potentially causing small blood clots and vascular constriction.

1.1.3. Burn Wound Progression

After initial thermal insult, the tissue necrosis process continues in the zone of stasis in burn wounds, a phenomenon called burn wound progression. It primarily results from the accumulation of free radicals and cytotoxic cytokines as well as the plugging of neutrophil in dermal venules as a consequence of prolonged inflammation (Figure 1). Edema formation with vascular congestion is abundant in burn wounds due to increased permeability of vessels and increased interstitial hydro static pressure. Blood flow is impaired through hypercoagulability and thrombosis, which also compromise vascular patency, as well as damaging the endothelial cells, which are the main differences compared to acute injuries[1].

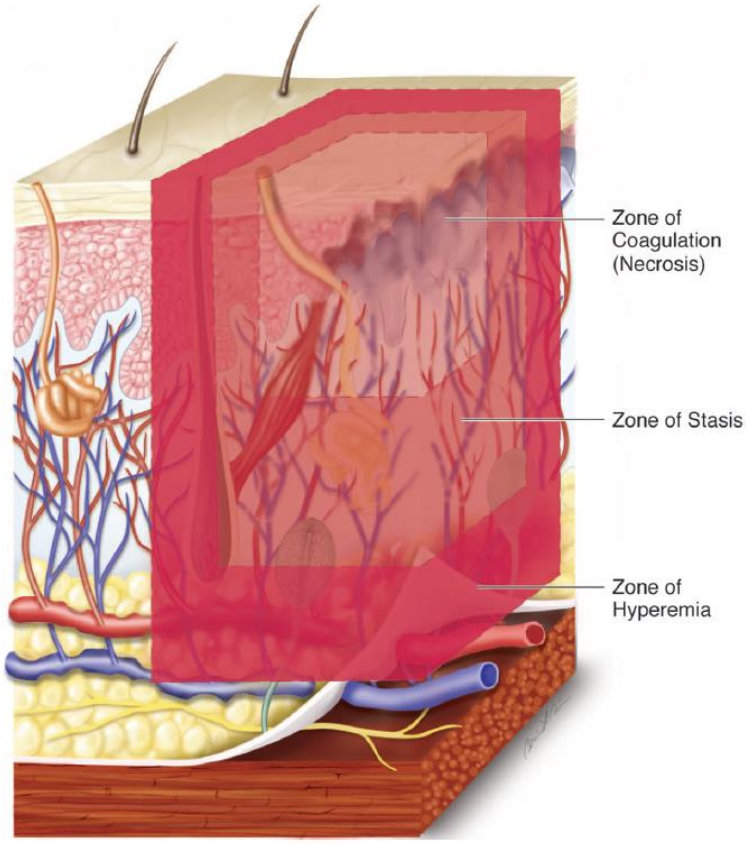

Figure 1. Thermal injury zones. The three zones of burn injury is illustraed as three-dimensional. (Reused from Ref.[1] with permission from Wolters Kluwer Group.)

1.2. Anatomy of the Skin

Skin has roughly 16,000 cm^2 area for adults and represents approximately 8% of the body weight with a very complex structure. The skin is traditionally layered into three regions: epidermis, dermis and subcutaneous tissue.

1.2.1. Skin Embryology

Skin is derivative of both the ectodermal and mesodermal layers of the embryo. The ectoderm is responsible for producing a stratified epithelial tissue and neuroectodermal elements such as melanocytes and skin neurons, while the mesoderm develops into sweat glands, sebaceous glands, and hair follicles [2]. Various cells and tissue elements are present in the dermal layer, including mast cells, macrophages, fibroblasts, Langerhan's cells (LCs), Merkel cells as well as lymphatic channels and blood vessels.

1.2.2. Epidermis

The epidermis is the outlying layer of the skin, of which thickness can vary according to the position in the body. For example, the thinnest epidermis occurs on the eyelids and is around half a millimeter-thick, whereas the thickest can reach 1.5 millimeters soles of the feet. There are 5 distinct layers of epidermis, which includes (from superficial to deep) the stratum corneum, stratum lucidum, stratum granulosum, stratum spinosum, and stratum basale. The epidermis is a metabolically active tissue. Cells found in the layer of stratum basale transmigrate superficially while they differentiate, and change their shape from columnar to planar in a process called *turn-over*. As keratinocytes migrate upwards, keratinocytes change their structures and physiological functions and their maturation is accompanied by the deposition of keratin and lipids. These cells eventually undergo apoptosis following their arrival at the *stratum corneum*, and this entire process, called keratinization, happens

continuously throughout life. No veins or capillaries is found in the epidermis, and nourishment and waste removal in this layer are mediated by dermal blood vessels located underneath. However, nourishment is able to reach only very bottom layers of epidermis leading to death of the cells found in the upper layers of the epidermis due to the lack of oxygen and nutrients.

Stratum corneum is the external layer of the epidermis, of which thickness ranges from 8–15 μm [3]. It consists of few layers of dead, hexagonal shaped, mature skin cells called corneocytes, which lack of most of their organelles and other internal structures and are filled with keratin fibers. These cells are also enclosed by intercellular lipids (mostly *ceramide*) which play a role in water retention [4]. They are also continuously discarded and replaced by cells migrating from lower parts of the epidermis.

Stratum lucidum is the sublayer beneath the *stratum corneum* consisting of dead, flattened cells which contains a clear intermediate form of keratin called as eledin. This material synthesized is main contributor to its "lucid" appearance. It assists decreasing friction between the stratum corneum and the stratum granulosum in the palms of the hands and soles of the feet.

Stratum granulosum is the distant layer in which living cells are found whose cytoplasm is filled with basophilic granules. The cells in this layer gradually lose their organelles, including nuclei and mitochondria, while accumulating keratin fibers and producing structures called lamellar granules that contain lipids and serve as a waterproof barrier. This barrier prevents evaporation, but also blocks the diffusion of nutrients into these cells, leading to their death in the outer layers on the keratinized epithelium.

Stratum spinosum consists of 10-20 layers of cuboidal cells (keratin-producing cells) that occur on basal cell layer. Basal cells flatten out these layers through the turn-over

process. The stratum spinosum is the thickest layer of the epidermis, typically ranging from 50–150 μm which is also known as squamous cell layer [3]. Cells found in this layer vigorously synthesize cytokeratin intermediate filaments anchored to desmosomes which join adjacent cells to maintain structural support and resistance against abrasion [5]. Langerhans cells are also found in this layer to help preventing infection.

Stratum basale is the deepest sublayer of the epidermis. In order to maintain cell turn-over, cells found in this layer constantly divide and provide new keratinocytes to be able to replace the ones that are continuously shed as they differentiate. Melanocytes are also found in this layer to produce the UV-protective melanin pigment [6].

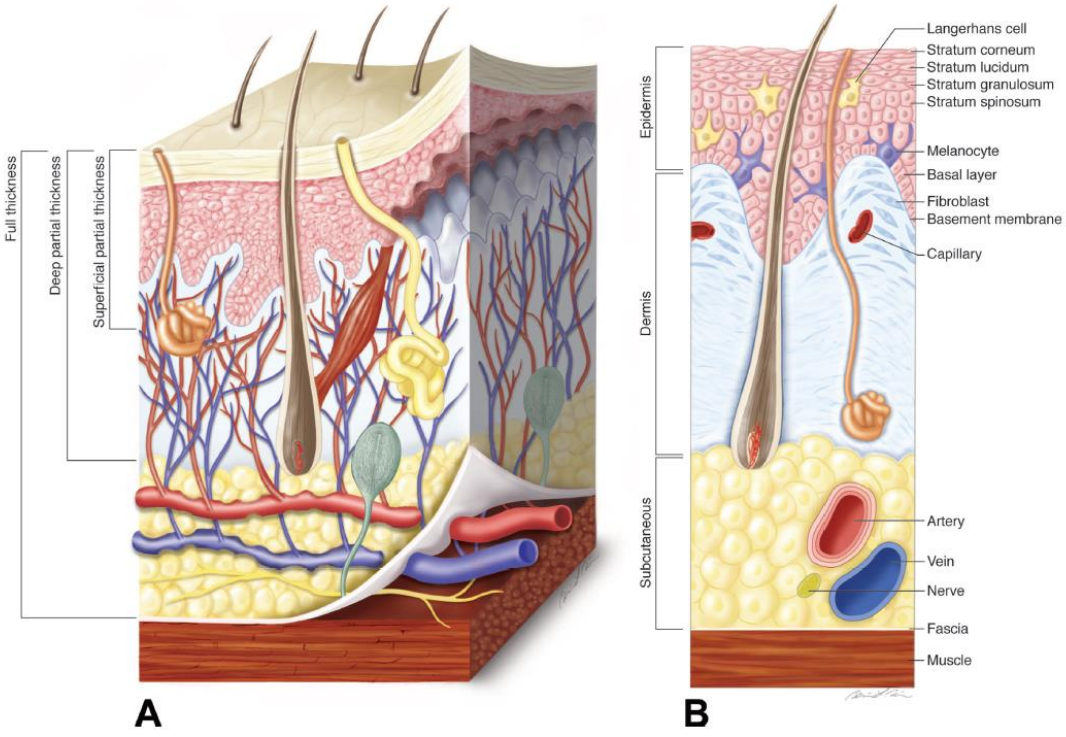

Figure 2. Skin Anatomy. A, Three-dimensional demonstration of the skin. B, Location of different cell types and important histological zones. (Reused from Ref. [1] with permission from Wolters Kluwer Group.)

1.2.3. Dermis

The dermis is the following main layer underneath the epidermis, and is considerably thicker (regularly 1-4 mm thick). Its thickness varies according to its position: on the eyelids it has 0.6 mm thickness; whereas on the soles of feet, it has 3 mm thickness. The dermis contains sub-epidermal structures such as connective tissue, elastic tissue, reticular fibers, and different specialized structures and cells including blood capillaries, nerve endings, apocrine and endocrine glands, sebaceous glands, hair follicles, lamellar corpuscles, and Meissner corpuscles. These sub-epidermal elements are responsible for transmitting the sensations of touch and pressure, as well as regulating the balance of salts and water in the dermal ECM. However, cells are generally sparser and protein fibers are more common in the dermis compared to the epidermis. All these proteins and molecules found in dermal layer contribute significantly to its density. Dominant structural components of the dermis are mainly produced and maintained by dermal fibroblasts, the strongly dominating cell type in the dermis. Mast cells and tissue macrophages also occur in this layer.

Collagen is an elongated, fibrous structural protein abundantly found in mammalian connective tissue and is a fundamental component of the ECM. It occurs as fibers and bundles, and contribute support for cell and tissue structures. Collagen is found all over the body, including cartilage, teeth, bone, tendons, ligaments and fascia and has important tensile strength. Collagen is also the most common structural component within the epidermis [7]. Collagen acts in a cooperative manner with elastin to maintain skin elasticity and strength by forming a mesh-like framework with blood and lymph vessels, fibroblasts and mast cells. These are surrounded by ground substance, consisting predominantly of glycosaminoglycans that enhance the water retaining properties of collagen and maintain humidity required in epidermis. The production

and maintenance of both collagen and elastin proteins are maintained fibroblasts, which are positioned primarily at the upper side of dermis. Collagen can also assist in tissue development by supporting blood vessels. Several unfavorable conditions can arise as a result of reduced production and turnover of collagen, such as aging symptoms including rhytids, loss of skin elasticity, and skin thinning. Collagen also significantly contribute to fat-free dry weight of skin. Type I collagen is the primary collagen in dermis and accounts for up to 80% of the collagen in skin, while Type III collagen accounts for another 15%, and the remaining 5% is mostly Types V and VI. There is a typical ratio between Type III and Type I collagen which is crucial to be maintained in scars after wound healing [8]. The dermis has the following two sublayers: reticular dermis and papillary dermis.

1.2.4. Papillary layer

Papillary layer is more superficial sublayer of dermis, which is contoured from the epidermis by ridges of papillae. These ridges are generally referred as rete pegs that increase the surface area of the dermal/epidermal junction and support the skin integrity. Wave-like border found in the dermis and epidermis promote the transfer of nutrients and oxygen between two layers. In aged skin, rete pegs are diminished and the surface area of the dermal-epidermal junction is decreased, resulting in the loss of sufficient nutrients and oxygen supply to the epidermis. For certain parts in the body, like hands and the feet that withstand the greatest frictional forces, having friction ridges and papillae is crucial since they enable to grasp objects as a result of friction. The fibers formed by elastin and collagen found in the papillary dermis create a finer network compared to those of the reticular layer and are arranged in a more disorganized fashion. This sublayer also contains a large amount of cells (*e.g.* fibroblasts), water, capillaries and nerve fibers [9].

1.2.5. Reticular layer

The reticular layer constitutes the lower part of the dermis and is found underneath the papillary dermis. This sublayer is denser and thicker than its more superficial counterpart (papillary dermis) and serve an uninterrupted transition to the subcutaneous layer. It includes fewer nerve fibers and capillaries but includes a high amount of elastic and collagenous tissue that are evenly distributed in an interwoven, crisscross pattern and aggregated into thick bundles in this layer [9].

1.2.6. Dermal Ground Substance

Ground substance consists of a broad range of anionic polysaccharides and glycosaminoglycans and is an integral part of the dermis and provides the necessary environment for the survival of dermal cells [10]. Heparan sulfate, dermatan sulfate, hyaluronates and chondroitin-4-sulfate form the ground substance in the skin, and the deposition of these substances is regulated by fibroblast and mast cells. The ground substance exists as a viscoelastic hydrogel of hydrophilic polymers and is responsible for water binding and flow resistance. Elastin and collagen, combined with non-fibrous substances like glycosaminoglycans (GAGs), altogether contribute the formation of ECM of this region. The vascular network is hard to replace following injury and plays a vital role in skin regeneration. Repair is delayed without adequate blood supply, and if adequate neovascularization cannot be accomplished in early state, scar formation is strongly enhanced at the wound site. Scar tissue has a several deficiencies that explain minimizing its formation when possible, although it is still preferable to non-healing tissue. With scar tissue formation, only 70% of tensile strength of the tissue can be recovered. Scars are also aesthetically disfiguring and not completely functional due to their undifferentiated state.

1.3. Important Elements Regulating Wound Repair Process

1.3.1. Growth factors

Initiation of the repair process in skin is quite complex and requires the action of several signaling cascade. Growth factors (GFs) are regulatory molecules involved in the activation of repair-associated signals under natural conditions. Growth factors can act in many different ways: they can be secreted endogenously to stimulate the cell itself (called autocrine signaling) or to communicate with other cells (called paracrine signaling). Stem cell research has made great progress in understanding the remarkable capacity of growth factors to elicit cellular behaviors such as differentiation, development, and regeneration; however, the action of various GFs are still not fully defined.

Delivery of growth factors to wound site is a problematic concept. Introduction of soluble growth factors into bloodstream is impractical and may cause systemic dispersion, which prevents the material from reaching necessary concentrations for initiating local repair. Three methodology have been established to efficiently deliver GFs to the site of injury. Firstly, DNA plasmid coding for a GF of interest can be utilized to allow its continued production at the wound site. Secondly, a GF-coding gene can be transfected to a cell type found in the skin, and these cells can then be supplied to the site of injury [11]. The last and most popular method does not require genetic intervention and entails the use of scaffolds as a carrier matrix to assist the delivery of growth factors. These scaffolds act as protective environments for GFs, preventing their degradation under *in vivo* conditions. However, the optimal release of GFs depends strongly on the degradation kinetics of the scaffold in tissue microenvironments.

Epidermal growth factor, vascular endothelial growth factor (VEGF), transforming growth factor-β (TGF- β) and fibroblast growth factor-2 (FGF-2) are commonly used GFs in the recovery of skin injuries [12]. Controlled release of GFs may enhance their activity as well as ensuring direct delivery. In previous studies, VEGF encapsulated in heparin peptide-based hydrogel scaffolds were able induce neovascularization in the cornea of rat eye, whereas these GFs were not effective in the absence of a scaffold matrix [13]. Likewise, vascular smooth muscle cells managed to synthesize more ECM in the presence of TGF-β1 immobilized in polyethylene glycol (PEG) hydrogel compared to the soluble TGF-β1 [14]. Carrier systems can be further functionalized with the addition of specific structures like glycosaminoglycan molecules to enhance their affinity to growth factors. Glycosaminoglycans (GAGs) are known to show affinity toward growth factors and prevent their degradation [15, 16]. In addition, growth factors carrying heparin binding domains (like VEGF-A or basic FGF (FGF-2)) can establish electrostatic interactions with GAGs through sulfate and carboxylic acid groups, and these binding interactions increase their stability [16-18]. Consequently, the use of heparin-mimetic molecules has gained considerable popularity in slow release studies during the recent decade.

1.3.2. The Extracellular Matrix (ECM)

Extracellular matrix (ECM) is composed of a broad range of proteins, proteoglycans, water and minerals, and forms the non-cellular part of tissues. Spatial and temporary organizations of signals arising from the ECM orchestrates the formation, function, homeostasis and regeneration of tissues by regulating cellular fates, and promoting the proliferation, migration, replication, differentiation or apoptosis of cells through molecules such as growth factors and pH modifications, and providing mechanical support to cells (Figure 3). The ECM contains different combinations of more than

100 types of molecules, the composition of which depends on tissue type, age and physiological conditions. The ECM contains molecules required for cell survival and differentiation and serves as a reservoir for soluble molecules such as cytokines, growth factors and chemokines, and consists of mainly fibrillary proteins, glycosaminoglycans and proteoglycans. [19-21]

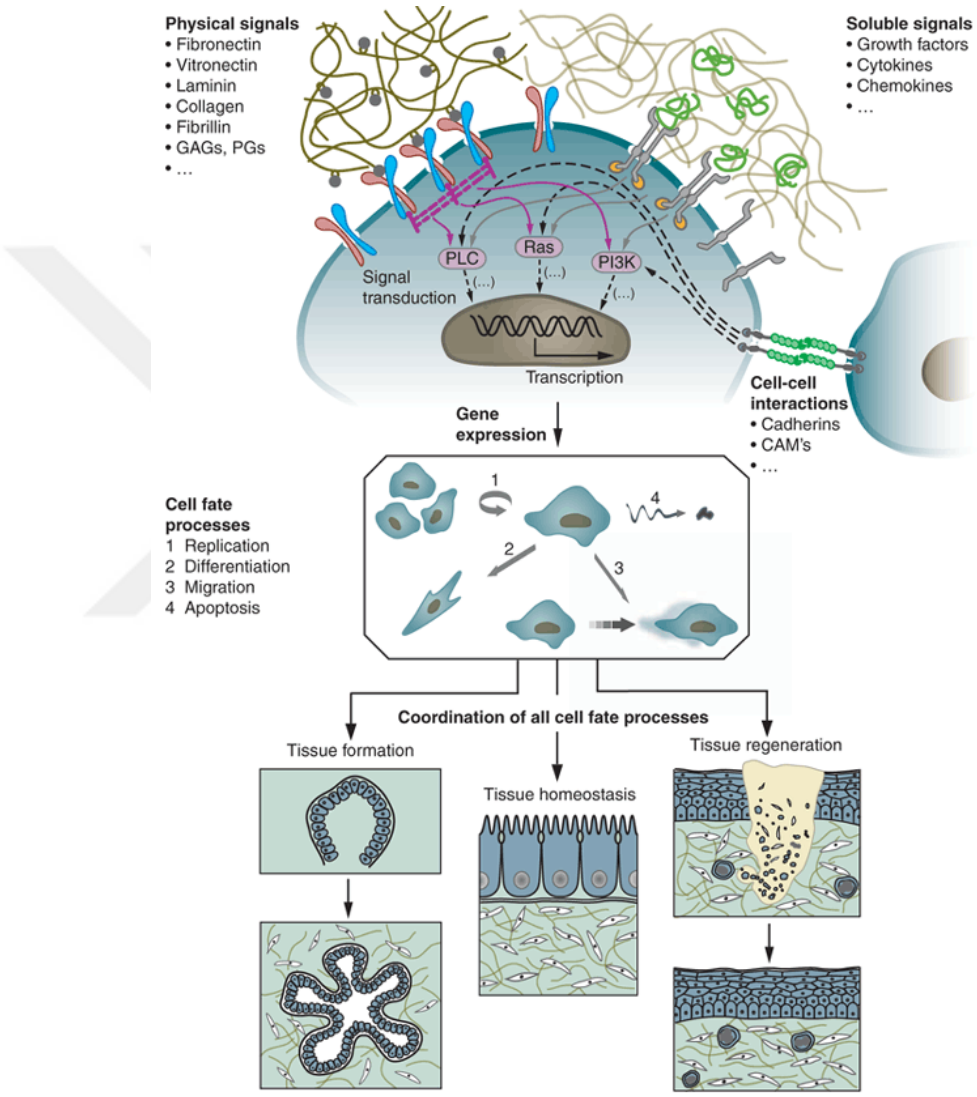

Figure 3. Dynamic interactions of cells with the surrounding ECM. Physical signals, soluble signals, cell fate processes and cell-cell interactions regulate processes such as tissue formation, tissue homeostasis and tissue regeneration. CAMs, cell adhesion molecules; PGs, proteoglycans; GAGs, glycosaminoglycans; PLC,

phospholipase C (Reused from Ref. [19] with permission from Nature Publishing Group).

Glycosaminoglycans and Proteoglycans

Proteoglycans are another class of ECM proteins and are heavily glycosylated. The basic unit of proteoglycan is consisting of glycosaminoglycan (GAG) chains that are bounded to a core protein in the middle [22, 23]. Due to their structure and composition, they can bind to certain cytokines and growth factors [24]. They are categorized as small leucine-rich proteoglycans (SLRPs), modular proteoglycans, cell-surface proteoglycans and according to the type of their GAG chain, core protein (nature of glycosaminoglycan chain), relative size and location [23]. GAGs are long, charged molecules and can be classified as sulfated and non-sulfated forms that consist of repeating units of disaccharide [galactose (4 N-acetylglucosamine-β1,3-galactose-β1), sulfated N-aceltylglucosamine or N-acetylgalactosamine, D-glucuronic or L-iduronic acid]. Sulfated GAGs involve heparin and heparan sulfate (consisting glucosamine and either glucuronic acid or iduronic acid), chondroitin and dermatan sulfate (consisting of galactosamine and either glucuronic acid or iduronic acid) and keratan sulfate (consisting of glucosamine and galactose). Non-sulfated GAGs are represented by hyaluronan, which doesn't bind to any core protein (Figure 4). GAGs can form highly hydrated structures and provide compressive strength to the tissues through their hydrophilic structures and ability to interact with water molecules [19].

GAGs are one of the most studied polysaccharides and have been shown to interact with cytokines, growth factors, ECM proteins and enzymes to modulate the microenvironments of cells. Consequently, they have substantial roles in various biological processes such as angiogenesis [25], neural development [26], cancer pathogenesis [27], anticoagulation [28] and embryogenesis [29]. Moreover, they are able to

direct signaling pathways by contributing to the formation of growth factor-receptor and enzyme-substrate complexes.

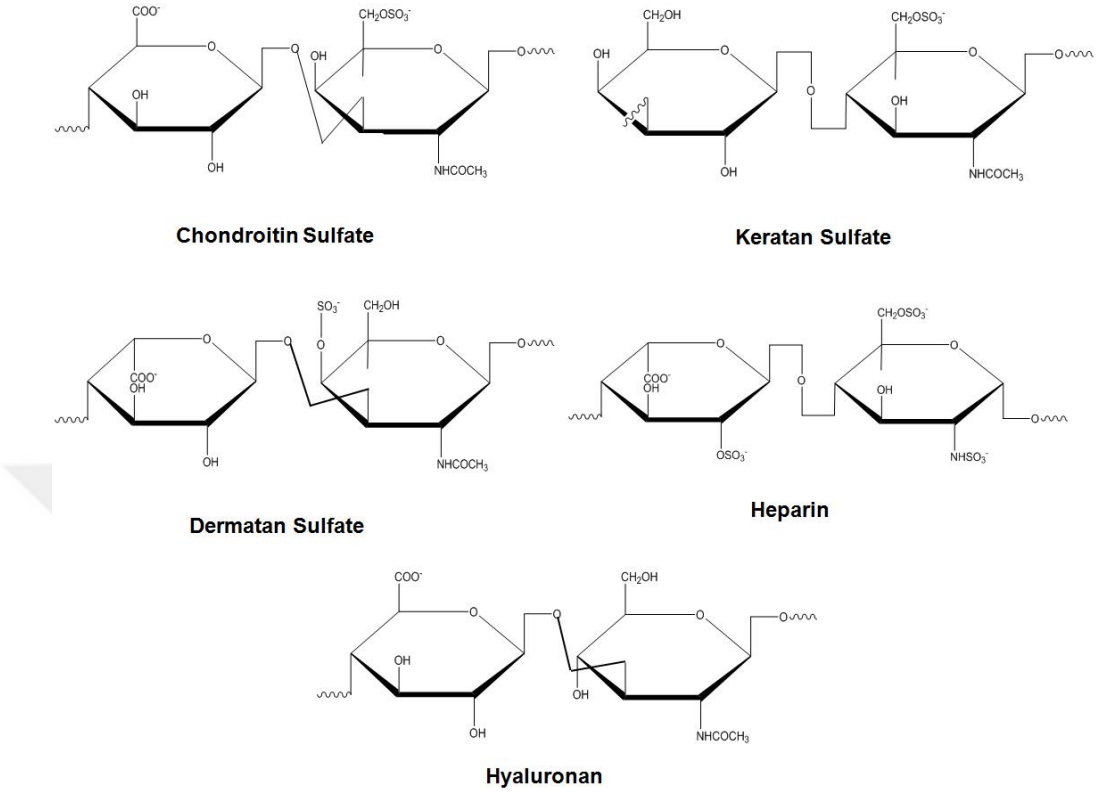

Figure 4. Glycosaminoglycans and their structural units.

1.4. Scaffolds

Scaffolds are defined as temporary platforms used for the cultivation of cells and tissues [30]. The efficiency and reliability of tissue engineering approaches heavily depends on the ability of scaffolds to provide cells with conditions (chemical and physical cues) that closely resemble their native environment. An ideal scaffold should allow intercellular communication of cells and exchange of nutrients, oxygen and waste products across the scaffold matrix through its porous structure. It should also facilitate the recruitment, proliferation and attachment of cells found at wound site and ensure the optimal differentiation and growth of the resident cell population by presenting biochemical signals and imitating the mechanical properties of skin

tissue [31]. ECM found in native tissue microenvironment meets all these criteria and has been extensively studied in tissue engineering.

Transplanting biofactors like cells, specific proteins such as small molecules, and their combinations within suitable scaffolds is a primary goal of regenerative medicine and tissue engineering. Biofactors carried within the structure of scaffolds can be used to initiate the repair process, while the porous, biocompatible, and degradable architecture of scaffolds imitates the volume and mechanical properties of the absent tissue [32, 33]. Although biomaterial design has achieved considerable progress, the clinical applications of biomaterials are currently limited and the development of next-generation systems is necessary for their use in medical settings. Several biomaterials authorized for treatment of in skin injuries by the Food Drug Administration (FDA), European Union (EU) or the German government[34] are shown in Figure 5. Generally speaking, the development of biomaterials that enhance the processes that are deficient at wound site is a promising way of repairing severe tissue injuries and serves as a viable alternative to organ transplantation.

Tissue	Product	Regulatory status	Description	Material						Cells		Use	Form
				Synthetic	Resorbable	Animal derived	Plant or bacteria derived	Human derived	Growth factor	Allogenic	Autologous		
Skin	TransCyte, Advanced Biohealing	1997	Nylon mesh coated with porcine collagen, containing non-viable human fibroblasts, with upper layer of silicon	✓	✓	✓				✓		Burns	Sheet
	Apligraf, Organogenesis	1998	Lower layer of human fibroblasts and bovine collagen, upper layer of keratinocytes		✓	✓				✓		Leg ulcers	Sheet
	Dermagraft, Advanced BioHealing	2001	Cryopreserved human fibroblasts on a polyglactin 910 (2-hydroxy-propanoic acid polymer with polymerized hydroxyacetic acid) mesh	✓	✓					✓		Diabetic foot ulcers	Sheet
	ICX-SKN, Intercytex	Phase II	Allogenic fibroblasts and human collagen with additional layer of keratinocytes		✓			✓		✓		Burns and acute wounds	Sheet
	Integra Dermal Regeneration Template, Integra Lifesciences	1996	Porous bovine collagen crosslinked with chondroitin-6-sulphate with upper layer of silicon	✓	✓	✓						Burns	Sheet
	Integra Flowable Wound Matrix, Integra Lifesciences	2007	Granulated bovine collagen crosslinked with chondroitin-6-sulphate		✓	✓						Ulcers	Gel
	Oasis Wound Matrix, Healthpoint	2006[a]	Decellularized porcine small intestinal submucosa		✓	✓						Burns, ulcers, other wounds	Sheet
	PriMatrix, TEI Biosciences	2008	Decellularized fetal bovine skin		✓	✓						Wounds	Sheet
	Xelma, Molnlycke	2005 EU	ECM protein (amelogenins) in propylene glycol alginate carrier		✓	✓	✓					Leg ulcers	Gel

Figure 5. Commercially available tissue engineering products for injuries and diseases of the skin. (Adapted from Ref. [34] with permission from Nature Publishing Group.)

Mimicking the three-dimensional (3D) composition of skin microenvironment is important for providing cells with a facsimile of their natural microenvironment. A 3D environment presented by biomimetic scaffolds allows the formation of replacement tissues by triggering cellular differentiation, and these platforms can be further enriched with small molecules and growth factors in order to enhance this process [35]. The incorporation of biological elements into the scaffold matrix is the main advantage of the biomaterial approach to wound recovery; however, these biological factors must be used in different combinations to effectively tackle each individual skin problem [12]. Consequently, optimization is an important aspect of biomimetic scaffold development.

1.4.1. Properties of scaffolds

A great variety of scaffolds have been developed to regenerate various organs and tissues in the literature. Although, there are no straightforward rules of thumb to describe how an ideal scaffold should be, a number of basic criteria must nonetheless be held by any biomaterial to effectively facilitate the regeneration process.

Biocompatibility is crucial for any scaffold, and it is imperative that neither the scaffold nor its degradation byproducts raise immune responses or produce toxic effects in the body. The healing process can be delayed due to immune responses, and the practical usability of scaffolds is decreased dramatically in the event of potential immunogenicity [36]. Scaffolds should also allow for cells to function in a manner analogous to their native environment, meaning that they shouldn't exhibit toxic, mutagenic or otherwise uncharacteristic activities.

Scaffolds should provide support to the site of injury until the recovery process is completed. They should ideally be eliminated through biological pathways, and their degradation and tissue repair should be synchronous to replace regenerating tissue gradually and smoothly.

Mechanical properties of scaffolds are another other key element in tissue engineering and should also be optimized to the tissue of interest. Scaffolds intended for regeneration of hard and ductile tissues, such as cartilage, bone, and cardiovascular muscle, should be particularly resistant to mechanical stress and able to provide support during the healing process. Production of scaffolds with non-ideal mechanical properties may also result in insufficient vascularization and cell infiltration [37].

Another crucial point for scaffolds in tissue engineering is a porous architecture, which enhances tissue regeneration by allowing the infiltration of surrounding cells into the scaffold at the site of implantation. The high metabolic demands of

proliferating cells at wound site can only be met through the adequate exchange of nutrients and gases. Pore size is critical for scaffold design to allow efficient cell binding, since cell communication relies on connections with the ECM through specific chemical groups. In addition, pores should be large enough to allow cell movements involved in recruitment and migration [38].

Lastly, the process of scaffold production is another point of interest. Since clinical use of scaffolds is generally the primary aim, the scaffolds should be designed to be reproducible, cost effective and commercially viable [38].

1.4.2. Types of Scaffolds Used for Regenerative Medicine

The primary aim of tissue engineering and regenerative medicine is to design biomaterials that provide optimized milieus for regenerating tissues. These materials can be divided into two categories: natural and synthetic.

1.4.2.1. Naturally Derived Biomaterials

Naturally derived materials carrying biological cues and native physical features are the first biomaterials to be used in clinical applications to provide a appropriate environment for the differentiation, proliferation, attachment and migration of cells [38]. These materials are exceptionally suitable for regeneration studies since they do not cause any toxicity and can be degraded by natural enzymatic systems in the host [12]. However, several concerns have been raised regarding their rapid degradation kinetics and potential to create inflammatory responses. The degradation kinetics of these materials can be altered through chemical modifications such as cross-linking; however, these functionalization processes may also be responsible for toxic effects [39].

Collagen, which can be obtained from both animal and human sources, is one the most prevalent proteins in the body and is the most studied natural molecule for tissue

engineering and regenerative medicine applications. Its degradation kinetics and pore size can be modified by altering its density[40]. Mechanical properties of collagen can also be modified by its combination with other synthetic materials [41]. Cell-ECM communications are primarily effected through the interaction of cell surface receptors and specific epitopes on soluble or ECM-bound biomolecules, which play crucial roles on the development of all organisms. These interaction can be replicated in biomaterial systems directly by the integrin family and the discoidin domain binding GFO (Gly-Phe-Hyp) motif, and indirectly with the RGD (Arg-Gly-Asp) sequence in fibronectin. [42-44] Indirect cell-collagen interactions, in which proteins containing the RGD motif bind to both integrins and collagen, are crucial for regulating cellular behaviors and is one reason for the efficiency of collagen scaffolds [45]. Effect of collagen-based scaffolds have been widely investigated in the regeneration of tissues such as skin [46-48], blood vessels [49], cornea [50], bone [51], cardiovascular system [52], urogenital system [53] and neural system [54].

Hyaluronan (hyaluronic acid) is a type of glycosaminoglycan that consists of β-(1,4) or β-(1,3) linked D-glucuronic acid and D-N-acetylglucosamine residues (Figure 4). Hyaluronan can be synthesized through bacterial production. It has exceptional water-holding capacity and viscoelastic properties. Hyaluronan is reported to be present in wound sites, vitreous chamber of the eye, and synovial fluid in joints, and has been shown to have important roles in cell migration, inflammation, fertilization, mitosis and angiogenesis [55, 56]. Hyaluronan has been shown to modulate chondrocyte proliferation, GAG and type 2 collagen synthesis [57, 58], cartilage histogenesis and cellular condensation in chondrogenesis [59]; as such, it is widely studied in cartilage regeneration. Hyaluronan based scaffolds have also been shown to contribute to bone regeneration when used to encapsulate the BMP-2 molecule [60]. This material has

several other applications in wound healing [61], nerve and brain regeneration [62] and reconstructive surgery [63].

Alginate is a polysaccharide that is the main component of seaweeds. It consists of β-(1,4) D-mannuronic acid and α-(1,4) L-guluronic acid [64]. Alginate, together with divalent cations such as magnesium and calcium, forms an ionotropic, elastic gel [65] that is biocompatible, injectable, and able to organize at physiological pH and temperature [66]. Mechanical properties of alginate gels can also be improved with $CaCO_3$ and $CaSO_4$ salts, but slow degradation kinetics is a major limitation of the system [67, 68] There are several applications of alginate in medical settings as a wound dressing [69] and for pancreatic islet delivery [70], cell mobilization [71], and cartilage tissue engineering [65].

Chitosan is a soluble derivative of chitin and has also been widely investigated for medical applications, since it exhibits properties such as antimicrobial activity, easy processability, biocompatibility, biodegradability, non-toxicity, and hemostatic potential [72]. Chitosan can be processed in a variety of forms, including hydrogels, fibers, sponges and membranes [73]. Due to these properties, chitosan is used extensively in wound healing [74], bone and cartilage regeneration [75], and nerve conduits [76].

Organ transplantation is associated with major problems involving organ failure and immunogenic effects. Organ rejection, which occurs due to antibodies found in the transplant recipient reacting with donor antigens, is one of the greatest limitations to organ transplantation and may force patients into taking immunosuppressive drugs for their entire lifetime. Decellularization is the process of removing native cells and isolating the ECM of tissue to enable the formation of scaffold materials. These scaffolds are able to enhance cell growth, differentiation and tissue development, and

can be recellularized with the patient's own cells to eliminate adverse immune responses. Consequently, decellularized matrices are commonly used in wound healing studies [77].

Apart from the aforementioned materials, several others have been reported for regenerative medicine and tissue engineering applications. These include fibrinogen [78], fibrin [79], silk [80], agarose [81], and dextran [82].

1.4.2.2. Synthetic Biomaterials

The natural environment supporting cells can be decellularized and utilized directly for tissue regeneration; however, these naturally derived materials are often immunogenic. This limitation has led to the development of synthetic materials that emulate the ECM environment with great accuracy while eliminating the batch to batch variance, zoonotic infection and immunogenicity problems associated with natural scaffolds [83]. The material properties of these scaffolds are typically engineered to fulfill the necesssary conditions for recovery of the tissue they are intended to replicate. This is a major advantage of synthetic materials, as it is relatively easy to control their immunogenicity, bioactivity, flexibility and degradation kinetics to optimally suit the tissue(s) of interest [84]. The FDA has approved the clinical use of biodegradable polyesters such as poly (lactic-co-glycolic acid) (PLGA), poly (glycolic acid) (PGA) and poly (lactic acid) (PLA), which are non-toxic and naturally degraded into equally non-toxic byproducts [85]. However, CO_2 is a degradation product of PLA and PGA, and may decrease the pH of environment and cause necrosis [86]. Several other polymers are also used in tissue engineering applications for different purposes, including polyphosphazenes for soft tissue regeneration [87], polyanhydrides for drug-delivery applications [88], and polyurethanes for vascular valves and grafts, prostheses and catheters [89]. Apart from the optimization of their mechanical and physical

properties, one the most challenging aspects of synthetic biomaterial design is to replicate the bioactive signals that modulate the attachment, migration, and differentiation of cells. Nevertheless, these materials can be modified with conjugation of *e.g.* peptide sequences to increase cell-integrin interaction [90]. Application of these synthetic molecules is also relatively less invasive and more site-specific thanks to their injectable properties [91].

Hydrogels made from synthetic molecules can harbor large amounts of water (up to thousands times their own dry weight), which strongly increases their biocompatibility [92]. PEG hydrogels are one the first examples of polymeric hydrogels and are formed through a cross-linking process that determines the mechanical properties and degradation kinetics of gel [88]. There are several applications of PEG hydrogels formed by photocross-linking in regenerative medicine, including encapsulation of pancreatic islets [93] and cells such as chondrocytes [94], osteoblasts [95], and mesenchymal stem cells, as well as the controlled delivery of nitric oxide to decrease the formation of thrombosis and restenosis [96].

Self-assembly is another process used in the formation of synthetic hydrogels. Rather than covalent interaction, this mechanism depends on the spontaneous assembly of a well-ordered system from a disorganized array of pre-existing molecules. Self-assembly is broadly seen in biological systems for macromolecular assembly, including the folding of proteins [97]. Non-covalent interactions such as hydrogen bonding, electrostatic interactions, van der Waals interactions, π–π stacking and hydrophobic-hydrophilic forces are responsible for the assembly process [98, 99]. Peptide amphiphile molecules have been described by Niece *et al.* as a new methodology to form a hydrogel containing nanofibrous structures at aqueous and physiological environments by combining two oppositely charged peptide amphiphile

(PA) molecules, which assemble through hydrophobic collapse and intermolecular noncovalent interactions in aqueous solution (Figure 6) [100]. Self-assembled peptide hydrogels are extensively studied in tissue engineering and regenerative medicine applications. Hydrogels formed by PA molecules can be degraded by enzymatic reactions and biological pathways, since they are mostly composed of amino-acid sequences [101]. Their porous and nanofibrous structures mimic the natural environment of the ECM. These PA materials can be modified to bear biological signals to replicate the structure of ECM. Apart from being inherently decorated biological signals and ligands, they are also able to carry and release small molecules and GFs in a controllable manner. Preclinical investigation of sell-assembling peptide amphiphiles have been performed for the regeneration of various tissues, such as heart muscle [102], nerve [103], cartilage [104] and bone [105], and also stem cell differentiation [106] and drug delivery systems [107].

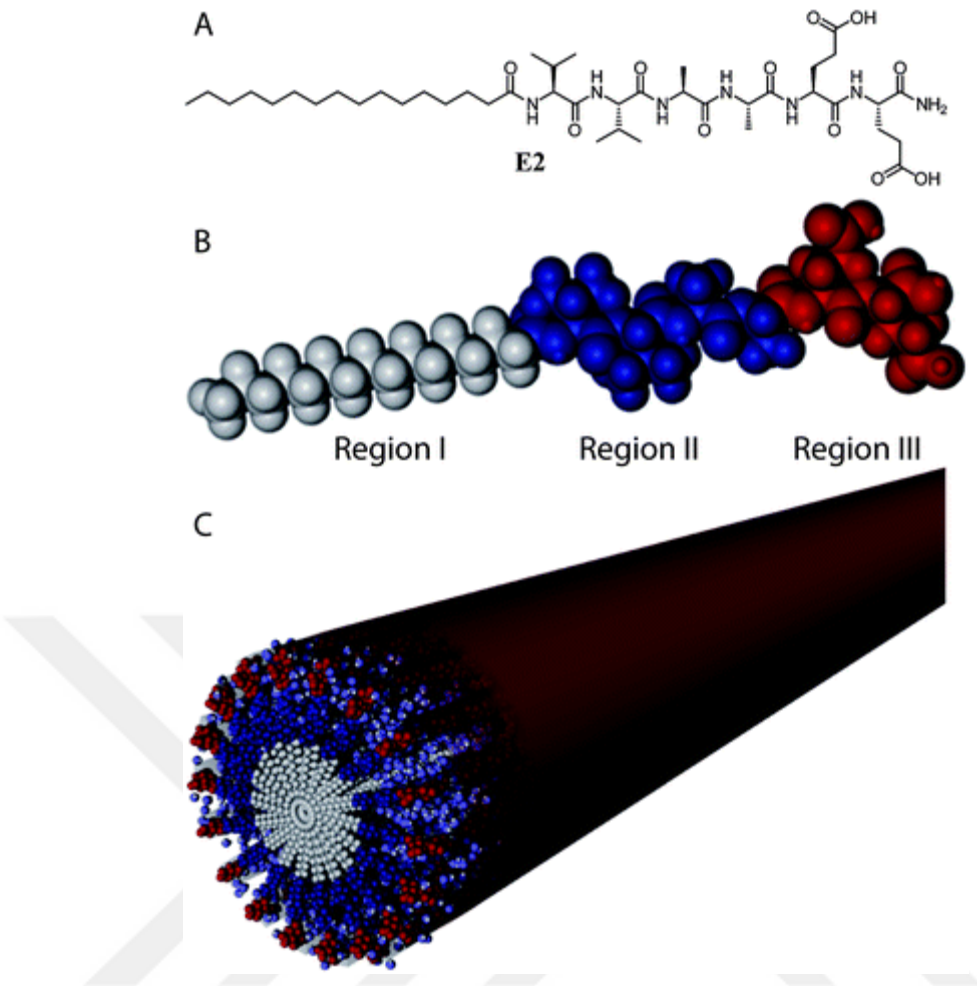

Figure 6. General structure and schematic representations of peptide amphiphile molecules and nanofibers. (A) Chemical structure, (B) different regions of structure, (C) nanofibrous structure of peptide amphiphiles (Reused from Ref. [108] with permission from Royal Society of Chemistry).

1.5. Angiogenesis, its Pathways, and its Mechanisms-of-Action

Angiogenesis is the physiological process in which the formation of new blood vessels are taking place from pre-existing networks. This process is orchestrated by complex biological signaling pathways that involve the participation of a broad range of molecules, including vascular endothelial growth factor (VEGF), fibroblast growth factor (FGF) and transforming growth factor β (TGF-β) [109]. Four main steps are achieved during angiogenesis; (1) endothelial cells are stimulated by angiogenic

factors, (2) capillary vascular basal lamina is degraded by activated endothelial cells, (3) a capillary sprout is formed and (4) vessels are matured through the migration of endothelial cells. The expression of VEGF is induced during early stages of angiogenesis and results in vasodilatation. Vessel permeability and downstream vascular leakage is increased through vascular permeability factor (VPF), which enables the extravasation of plasma proteins (such as plasma-clotting proteins and fibrin/fibrinogen) and induces the formation of a fibrin mesh that provide a temporary matrix for migration of endothelial cell. This regulation of vascular permeability is necessary to prevent the excessive loss of plasma proteins. A protein called Angiopoietin-1 (Ang1), which is the ligand of the endothelial receptor Tie-2, increases the stability of newly formed vessels and protects existing vessels from leakage. Ang1 and VEGF work synergistically during the development of vessels.

The second stage of neovascularization requires the migration of endothelial cells, which is achieved by the proteolytic degradation of ECM components and basement membrane through enzymes called matrix metalloproteinases (MMPs). Their proteolytic activity is regulated by tissue inhibitors of metalloproteinases (TIMPs). Among all MMPs, MMP2 (gelatinase A) and MMP9 (gelatinase B) play the most crucial roles for angiogenesis by degrading the collagen that is found in the vascular basement membrane. Other MMPs also have important roles in different pro- and anti-angiogenic processes.

Degradation of the basal lamina facilitates the chemotactic stimulation of endothelial cells, which migrate and proliferate through the activity of factors such as EGF, bFGF, angiopoietins, and chemokines. Following this process, endothelial cells either assemble into tubular structures in the ECM or merge with existing vessels to establish new ones.

The vessel maturation step requires the deposition of a vascular basement membrane and recruitment of periendothelial cells, which increase the stability the newly formed vessels by inhibiting further proliferation and migration of endothelial cells through the formation of pericyte-endothelial associations. A great number of growth factors and inhibitors are involved in regulating the angiogenesis process: Platelet growth factor (PDGF), fibroblast growth factor (FGF), hepatocyte growth factor (HGF), hypoxia-inducible factor (HIF) and vascular endothelial growth factor (VEGF), and are known as angiogenic (stimulatory) GFs, while thrombospondin, angiostatin, angiopoietin, endostatin, interferon and pigment epithelium-derived factor (PEDF) are recognized as angiogenic inhibitors [110]. A very precise balance of these factors is necessary for the establishment of healthy new blood vessels, and the disruption of this balance can cause abnormal blood vessel growth and insufficient vessel formation. Both effects are broadly seen in many diseases.

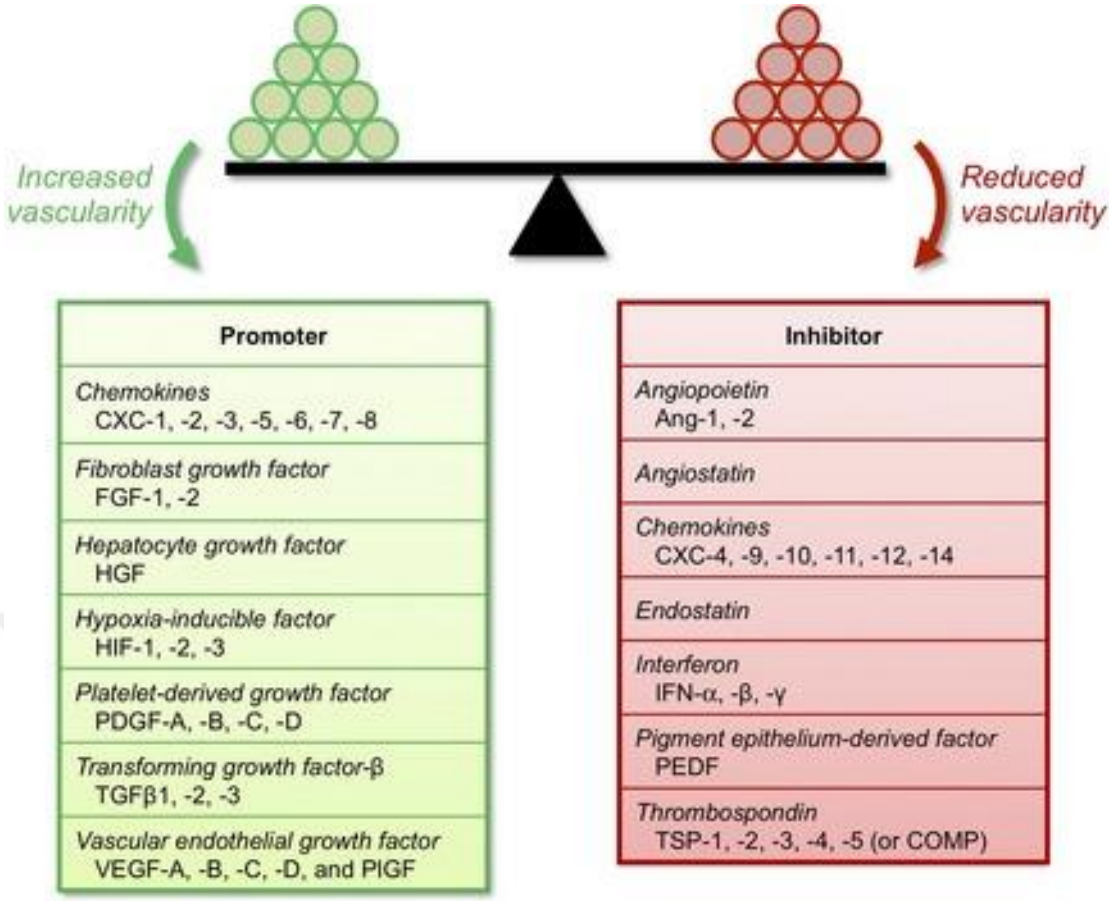

Figure 7. Regulation of angiogenesis process trough pro-angiogenic factors and anti-angiogenic factors (Reproduced from Ref. 1 with permission from Journal of Cellular and Molecular Medicine [110]).

Apart from being associated with different diseases, angiogenesis is also required for healthy wound healing, since granulation tissue formation and the transportation of nutrients and oxygen are heavily dependent on newly formed blood vessels. Angiogenesis is rapidly induced in response to injury through the action of various cells (i.e. macrophage, monocytes), growth factors (vascular endothelial growth factor, angiopoietin, fibroblast growth factor, and transforming growth factor beta), cytokines and extracellular matrix (ECM) components. A high functional redundancy is assumed in this process, since a complex network of numerous mediators are involved in angiogenesis.

1.5.1. Role of Angiogenesis in Wound Healing

Requirement for oxygen and nutrients is dramatically high in wound area because of injury-induced disruption in blood vessels. Therefore, it is critical to restore blood flow to the site of injury to support the viability, differentiation and proliferation of native cells and maintenance of cytokines [111]. Impaired angiogenesis has also side effects on the functions of ECM components, keratinocyte migration and proliferation, granulation tissue formation, collagen deposition and macrophage function [112].

As described previously, multiple steps must be achieved for a successful angiogenesis process, including vasodilation, degradation of basement membrane, migration and proliferation of endothelial cells. Immediately after tissue damage, a clot is formed through the action of thrombin, and VEGF expression is strongly upregulated. Activation of other angiogenetic growth factors like PDGF, angiopoietin-1 (Ang-1), TGF-α and TGF-β is facilitated by platelet cells. Therefore, the main initiators of the angiogenesis process are thrombin and platelet cells. Afterwards, angiogenesis is amplified through the action of monocytes and macrophages, which release growth factors and pro-inflammatory cytokines in order to enhance blood flow to the site of injury. Absence of blood circulation also causes hypoxic conditions, in which the expression of HIF-1α is upregulated and VEGF expression is also enhanced. The stabilization of newly formed blood vessels is then modulated by Ang-1, alpha-smooth muscle actin (α-SMA) and PDGF. Pericytes are recruited to newly formed vessels with the last of these factors, and guide both the sprouting process and maturation of vessels [101]. Lastly, blood vessel formation is suppressed at the final stage of angiogenesis, which is characterized by the upregulation of endogenous angiogenesis inhibitors (Figure 8).

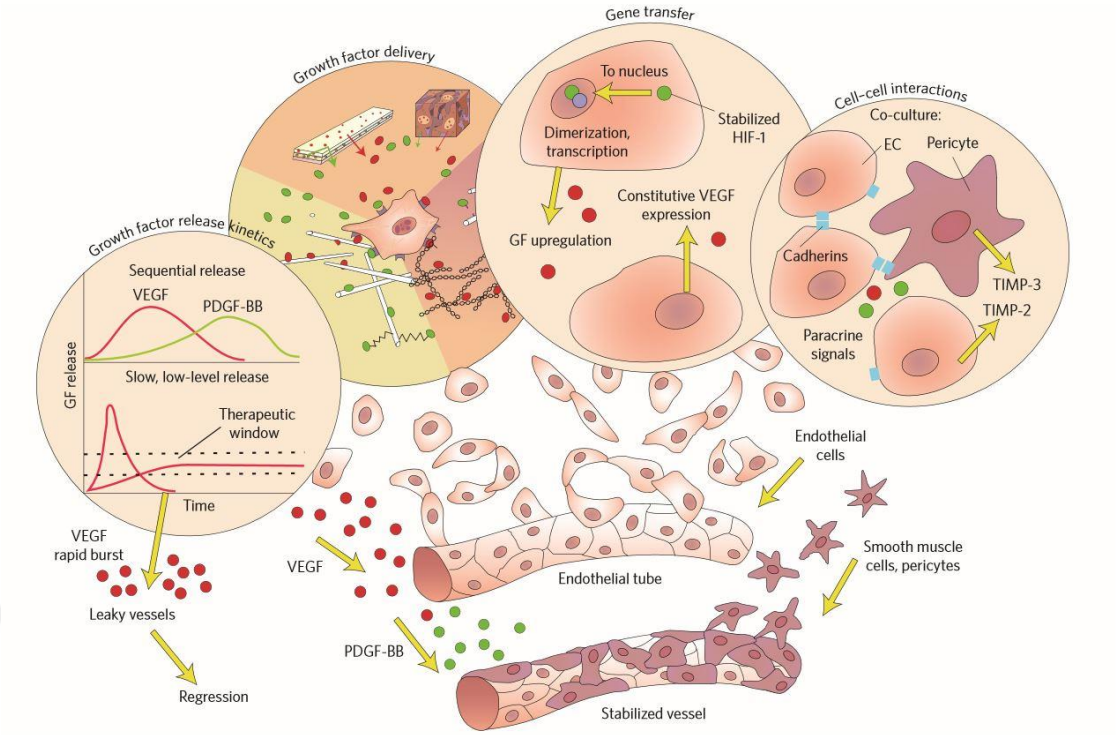

Figure 8. Vascularization of tissue-engineering scaffolds. (Reused from Ref. [19] with permission from Nature Publishing Group).

1.5.2. Biomaterial-Based Therapeutics to Target the Angiogenesis Process

Protein and peptide-based therapies designed to stimulate or inhibit angiogenesis have been clinically tested for a decade; however, only a few therapeutic agents have been approved. Transition of angiogenesis therapy from animals to humans requires comprehensive animal studies with biomaterials-based systems, which are currently limited. However, biomaterials nevertheless show great promise and might emerge as a new platform for the treatment of diseases which are currently known to be unresponsive to clinical intervention.

The discovery of advanced synthesis methods has facilitated the development of a great number of therapeutic reagents and peptide-based drugs. The development of synthetic peptides has progressed considerably with solid-phase peptide synthesis

especially in the areas of biotechnology and medicine. Among peptide based biomolecules, peptide amphiphiles are very useful to develop materials with advanced multi-functional properties through simple chemical alterations. Solid-phase peptide synthesis and liquid-phase peptide synthesis are two main methods commonly used in peptide based biomaterials. Solid phase peptide synthesis method depends on the progressive addition of amino acids onto an insoluble resin. After the first amino acid is attached to resin by a linker, following amino acids are added from the carboxy-terminus to the amino-terminus. Side chains of each amino acid are bound to protecting groups to prevent any undesirable reaction throughout chain assembly. Protected groups are then removed in a controlled manner in each coupling reaction until the chain is completed. Finally, the synthesized peptide is cleaved from resin and lyophilized. The purity of the peptide molecule can be evaluated by liquid chromatography and mass spectrometry. The peptide can also be purified reverse-phase high-performance liquid chromatography [1].

The optimum length of peptide molecules for scaffold applications is between 10-20 amino acids. Larger peptides typically show solubility and uptake problems, limiting the maximum size that is feasible for use in cellular applications. Chemical structure of certain amino acid sequences complicate synthesis efforts, but in general, hydrophilic sequences are more soluble and known to be easier to synthesize. Peptides can be synthesized either manually or through a peptide synthesis machine. Although the manual methodology requires significant knowledge of peptide chemistry and is labor intensive, it allows much greater flexibility in the design and modification of peptides.

Peptides have favorable properties over antibodies in terms of their solubility, cost, size, and ease of modification and manufacturing [113]. Since the angiogenesis process

entails the actions of multiple targets and regulators during proliferation, migration, tube formation and vessel maturation, those regulators can be targeted with peptide-based strategies to induce or inhibit angiogenesis. There have been many attempts to develop angiogenic modulators, generally targeting two molecular systems: VEGF (or its receptor) and integrin. A proline-rich, 39 amino-acid long peptide called PR39 was found to trigger angiogenesis by protecting HIF-1α from ubiquitin–mediated degradation in proteasomes and upregulating its expression, which activates several genes that promote survival in low-oxygen conditions [114]. SVVYGLR is derived from the sequence of osteopontin, which is another peptide-based angiogenic stimulator sequence [115]. The arginine-glycine-aspartic acid (RGD) sequence is a primary recognition site between ligands and receptors that is found in many ligands, and is involved in cell adhesion. This bioactive sequence was used for the delivery of doxorubicin to endothelial cells, which results in the inhibition of tumour growth and metastasis in mice [116]

1.6. Self-assembled peptides in wound repair and regeneration

Skin provides a protective interface against microbial invasion, prevents water loss through evaporation, and hosts a range of sensory receptors for the detection of temperature and mechanical stimuli [117]. The physical integrity of skin is therefore essential for its function, and skin wounds are characterized by the rapid restoration of this integrity at the expense of fine structural details: Skin appendages and sensory corpuscles, for example, are produced only at the final stages of recovery, and recently repaired skin wounds contain an extracellular matrix environment that is mechanically and biochemically distinct from healthy tissue. One consequence of this rapid-but-incomplete repair is the creation of long-lasting fibrotic scars, which fail to regain the level of functionality present in unwounded skin [118]. In addition, large-area

laceration and burn injuries are beyond the capacity of myofibroblasts to close and repair under short time scales, resulting in an increased risk of secondary infections during recovery. Due to the shortcomings inherent to the natural skin regeneration process, many efforts have been made to enhance the recovery of skin wounds through the use of cell or tissue grafting techniques, natural or artificial scaffolds, and bioactive molecules such as growth factors and immunoregulatory elements; all of which aim to modulate the vast network of signaling pathways that characterize wound repair in eukaryotic systems [119].

Wound healing is a complex and continuous process that occurs through an extensive series of well-regulated interactions between cells, extracellular elements, and signaling molecules present at the site of injury [120]. In general, however, the recovery of skin wounds can be classified under four distinct stages: hemostasis, inflammation, proliferation and remodeling [118, 121]. The hemostasis stage begins immediately following wounding and involves the cessation of bleeding through vasoconstriction, formation of a fibrin-based wound clot through coagulation and the initial recruitment of immunoregulatory cells to the injury site. Following this step, the recruited immune cells raise a local inflammatory response and clear the wound bed of debris and invading bacteria, while secreting growth factors that stimulate the proliferation and differentiation of keratinocytes, fibroblasts and endothelial cells. These cells in turn are responsible for depositing new extracellular matrix elements, mediating the contraction of the wound, and producing new blood vessels to supply the healing tissue with oxygen and nutrients. Lastly, the healing tissue gradually matures over the following weeks through the resorption of excessive blood vessels, development of new skin appendages and sensory elements, and the replacement of type-III collagen with a well-crosslinked type-I collagen network [122, 123].

Acute wound injuries are typically treated using commercially available wound dressings, which prevent bacterial entry, hydrate the wound site, and may be functionalized with growth factors, antioxidants, vitamins or antimicrobial agents to further enhance wound recovery [124]. In addition, natural and synthetic materials are widely used for the development of hydrogel scaffolds in regenerative medicine and tissue engineering, with a great number of applications reported for the recovery of skin wounds in particular [125]. However, these materials may exhibit low biocompatibility, raise strong immune responses, or give rise to toxic degradation products under *in vivo* conditions, necessitating the development of more advanced biomaterial hydrogels for wound repair [12, 126]. Self-assembled peptide systems have emerged as one alternative approach for the development of biocompatible scaffold materials, and are particularly promising in this context due to their ability to be functionalized with a broad range of bioactive signals. These signals can stimulate cellular recruitment, adhesion, differentiation and proliferation to regulate the behavior of cells at the site of injury and, due to their biological origins, prevent the creation of unwanted immune responses against the scaffold and/or the cells it contains [19, 66, 127].

RADA16 (RADARADARADARADA) is one of the most common peptide sequences used for the treatment of skin injuries, and readily self-assembles into well-organized β-sheet structures in water [128]. While self-assembled peptide scaffolds are typically designed to mimic the structure of a particular protein, RADA16 has been developed purely for its structural properties and does not contain bioactive motifs, although the sequence bears some similarities to the fibronectin-derived, adhesion-promoting RGD motif. Chirality also appears to be important for the biofunctionality of this peptide sequence, as L-RADA16 peptide hydrogels are able to mimic cell

microenvironment and enhance cell proliferation, while the D-form peptide hydrogels induce cell growth and rapid hemostasis [129, 130]. Despite its lack of bioactive motifs, the sequence has been successful in mediating the repair of skin wounds: RADA16-I, a derivative of RADA16, has been shown to increase the rate of repair by 20%-30% in second-degree burn injuries compared to blank controls and miscellaneous wound dressing scaffolds (chitosan, collagen I and PDLA) [131]. The base RADA16 sequence has also been used in conjunction with human fibroblast cells and keratinocytes to develop a synthetic skin in the absence of any biologically-derived materials [132], while another, shorter peptide sequence (LIVAGKC) was found to stimulate enhanced reepithelialization in a full-thickness porcine excision wound model [133].

In addition to directly participating in signaling pathways through their physical structures and amino acid sequences, self-assembled peptide hydrogels can also carry cargos of other bioactive molecules. Bioactive mediators such as cytokines and chemokines play important roles in regulating the interactions between cells and biomaterials in drug and protein delivery, tissue regeneration and cell culture applications, and the efficiency of the peptide material in promoting a particular cellular response can be enhanced through their delivery within the self-assembled scaffold [12, 126, 134-136]. For example, functional proteins such as vascular endothelial growth factor, fibroblast growth factor, brain-derived neurotrophic factor, lysozyme, trypsin inhibitor, BSA, and IgG have been integrated into RADA16 peptide hydrogel scaffolds without losing their original structure and functions [136, 137]. In particular, Schneider *et al*. reported that the release of epidermal growth factor (EGF) by a RADA16-I scaffold is responsible for enhancing wound coverage by 5-fold compared to untreated controls on an *in vitro* human skin tissue model, and EGF release from the scaffold was found to selectively occur in the presence of the skin model, but not

in PBS [138]. In addition to scaffold structures, a chimeric keratinocyte growth factor/elastin fusion protein has been reported to self-assemble into nanoparticle-like aggregates and promote re-epithelialization and granulation by 2-folds and 3-folds in a diabetic mouse model [139].

While peptide molecules can undergo self-assembly through their structures alone, their assembly behavior is often promoted by appending a hydrophobic tail region at one end of the peptide sequence. The result of such a modification is a new class of molecules called *peptide amphiphiles*, which have been used with increasing popularity in tissue engineering applications during the past decade. Peptide amphiphile (PA) molecules can be designed to self-assemble either by themselves (through hydrophobic and hydrophilic interactions) or in the presence of an oppositely-charged peptide amphiphile molecule (through charge neutralization between charged residues), producing hydrogel scaffolds with the biocompatibility, non-toxicity, non-immunogenicity and sequence-specific biological activity inherent to peptide molecules. As with peptide-only nanostructures, the water-rich hydrogel structure of PA scaffolds is highly amenable for the controlled release of growth factors and other bioactive molecules. Consequently, the use of peptide amphiphile hydrogels has been described for a wide range of wound-related applications, including the promotion of collagen release from human fibroblasts using the palmyl-KTTKS sequence and the promotion of angiogenesis by the palmitoyl-LRKKLGKA [140] and basic fibroblast growth factor-loaded palmyl-AAAAGGGERGD sequences [141].

A heparin-mimetic peptide sequence (HM-PA, lauryl-VVAGEGDK(*p*-benzosulfonate)S-Am) was also developed by our group for a variety of applications and exhibited some potential for use in wound healing. This peptide amphiphile

sequence is incapable of self-assembling by itself, but undergoes charge neutralization with a negatively-charged PA molecule (typically E-PA, lauryl-VVAGE) to form hydrogel scaffolds exhibiting strong affinity towards a range of growth factors [142]. The HM-PA/E-PA mixture was shown to stimulate angiogenesis, re-epithelization and granulation tissue formation compared to a sucrose control in an acute full-thickness rat skin wound model, with an additional (albeit non-significant) trend for increased skin appendage formation [118]. This PA system also displayed similar results in a diabetic rat model, effectively modulating the dysfunctional immune responses and extended recovery period associated with diabetic wounds [143]. In contrast to the bioactive scaffold, the presence of non-bioactive control networks (containing a mixture of E-PA and the positively-charged K-PA (lauryl-VVAGK) molecules) did not significantly affect the diabetic wound healing process, suggesting that the immunoregulatory and growth-stimulating effects of the PA scaffolds were sequence-specific. The affinity of this scaffold towards endogenously produced growth factors, as well as its general similarity to cell-regulating glycosaminoglycan molecules, are possible reasons for this behavior.

CHAPTER 2

A HEPARIN-MIMETIC PEPTIDE AMPHIPHILE ENHANCES THE RECOVERY OF FULL-THICKNESS BURN INJURIES

This work is partially described in the following publication[144]:

Fatih Yergoz[1],, Nurcan Hastar[1], Cagla Eren Cimenci[1], Alper Devrim Ozkan[1], Turgay Tekinay[2], Mustafa O. Guler[1, 4], * , Ayse B. Tekinay [1,2,3], *

[1]Institute of Materials Science and Nanotechnology, National Nanotechnology Research Center (UNAM), Bilkent University, Ankara, 06800, Turkey

[2]Life Sciences Application and Research Center, Gazi University, Ankara, 06830, Turkey; Department of Medical Biology and Genetics, Faculty of Medicine, Gazi University, Ankara, 06500, Turkey

[3]Neuroscience Graduate Program, Bilkent University, Ankara, 06800, Turkey

[4]Institute for Molecular Engineering, University of Chicago, Chicago, IL 60637 USA

*Corresponding author

E-mail addresses: mguler@uchicago.edu (Guler, M.O.), atekinay@bilkent.edu.tr (Tekinay, A.B.)

2.1. Introduction

Burn injuries are the fourth most common type of trauma worldwide, and third-degree burns constitute one of the most severe injuries of the skin. Although, recent developments in post-injury care have greatly improved the survival and recovery rates of patients suffering from severe burns, the considerable length of the recovery process and the concurrent risk of infection contribute to patient mortality in burn injuries [145]. Even under ideal conditions, the formation of scar tissue follows wound closure, and may compromise the appearance and functionality of the healed tissue [146]. In addition, burn wounds are subject to a higher risk of necrosis compared to lacerations and blunt trauma injuries due to the oxidative and inflammatory stresses exerted by the zone of coagulation [1, 147]. Consequently, untreated burn injuries often experience a period of progression where viable tissues adjacent to necrotic regions are themselves converted into necrotic tissue, increasing the depth and diameter of the injury [148, 149]. Severe burn injuries are also associated with a rapid and systemic immune response that may result in septic shock, caused by a combination of increased capillary permeability, an excess of proteins in the interstitial space, and the overexpression of pro-inflammatory factors by macrophages [150]. Taken together, these factors necessitate the development of novel techniques that specifically address the unique pathophysiological needs of burn injuries, especially with regards to the ability to halt burn wound progression and facilitate tissue repair with minimal scar formation [151].

Hydrogels are effective materials for treatment of burn injuries, because they provide an environment similar to one present in native skin tissues, retaining water and modulating the fluid balance at the site of injury. They can be functionalized with bioactive or antimicrobial agents to prevent secondary infections or accelerate the

wound repair process [146]. Self-assembled peptide nanofiber gels contain bioactive sequences that effectively replicate the functions of many extracellular matrix proteins, allowing their use for the repair of a broad range of tissue injuries [152-154]. Previously, peptide gels were used as wound dressings for both burn and laceration injuries [155, 156]. We recently reported that heparin-mimetic peptide nanofibers (HM-PA, Lauryl-VVAGEGD(K-psb)S-Am) increase re-epithelialization and granulation tissue formation in a rat acute skin wound model [118]. In contrast, non-bioactive control gel (bearing a similar secondary structure but no heparin-mimetic motifs) provided no improvement over sucrose-treated controls, suggesting that the sequence (rather than the presence of the gel as a scaffold) was effective in promoting wound healing, possibly through the selective retention of growth factors by HM-PA [13].

In the present study, we show that HM-PA nanofiber gels facilitate recovery of burn injury caused by a thermal burn model developed for the evaluation of topical treatment methods. Wound regeneration was monitored through histological observations, immunostaining and marker protein expressions across 21 days of recovery, and blood vessel densities, collagen organization and skin appendage formation were quantified to determine the effect of bioactive PA treatment on the repair process. The HM-PA treatment was observed to enhance angiogenic activity during early regeneration; increase wound closure, re-epithelialization and granulation tissue formation rates and promote the formation of skin appendages compared to saline treatment and 3M™ Tegaderm™ wound filler suggesting that the HM-PA gel can be utilized as an ideal potential platform for the treatment of burn wounds in addition to laceration injuries.

2.2. Materials and Methods

2.2.1. Materials

9-Fluorenylmethoxycarbonyl (Fmoc) and tert-butoxycarbonyl (Boc) protected amino acids, lauric acid, 4-(2′,4′-dimethoxymethyl-Fmoc-aminomethyl)-phenoxyacetamido-norleucyl-MBHA resin (Rink amide MBHA resin), Fmoc-Asp(OtBu)-Wang resin, 2-(1H-benzotriazol-1-yl)-1,1,3,3-tetramethyluronium hexafluorophosphate (HBTU) and diisopropylethylamine (DIEA) were purchased from NovaBiochem (Merck) and all other chemicals were purchased from Sigma-Aldrich, Thermo scientific, Invitrogen and Fisher. Antibodies used in this study were purchased from Millipore and Abcam.

2.2.2. Synthesis and Purification of Molecules and Gel Formation

Fmoc solid phase peptide synthesis method was followed for the synthesis of peptide amphiphile (PA) molecules. Two different solid supports were used according to the charge of the PA molecule to be synthesized: Positively-charged PAs, (HM-PA (Lauryl-VVAGEGD(K-psb)S-Am) and K-PA (Lauryl-VVAGK-Am)), were fabricated using Rink amide MBHA resin, while the negatively-charged PA (E-PA (Lauryl-VVAGE)) was synthesized on Fmoc-Glu(OtBu)-Wang resin. Coupling of each amino acid residue was performed through the activation of carboxylate groups of two equivalents of Fmoc protected amino acids with 1.95 equivalents of HBTU and 3 equivalents of N,N-diisopropylethylamine (DIEA) for 1 mole equivalent of starting resin for 3 h. In each step of amino acid coupling, samples were treated with 20% piperidine/dimethylformamide (DMF) solution to remove Fmoc protecting groups on amino acids. Remaining free amine groups were permanently acetylated and blocked with 10% acetic anhydride solution in DMF after each amino acid coupling. DMF and dichloromethane (DCM) were used as washing solvents after each step and used to wash away excess chemicals in the reaction mixture. In the synthesis of sulfonated

PA, HM-PA (Lauryl-VVAGEGD(K-psb)S-Am, the side chain of the lysine was conjugated to *p*-sulfobenzoic acid, which was protected with Mtt (4-methyltrityl) for the selective deprotection of amine groups under subsequent steps. Before the coupling of *p*-sulfobenzoic acid to the lysine residue, the Mtt protecting group on the lysine side chain was removed by shaking the resins with a cocktail solution of trifluoroacetic acid (TFA):triisopropylsilane (TIS):H_2O:DCM at the ratio of 5:2.5:2.5:90 for 5 min. The cleavage of synthesized PA molecules from solid support resin was then carried out with a cocktail solution of TFA:TIS:H_2O at a ratio of 95:2.5:2.5 for 2 h. Excess chemicals (mainly TFA and DCM) were removed by rotary evaporation. The viscous PA solution was then precipitated with ice-cold diethyl ether at -20 °C overnight. The resulting white precipitate was collected through centrifugation and dried under vacuum. The precipitate was then dissolved in ultrapure water and left frozen at -80 °C overnight. On the following day, the frozen solution was collected and lyophilized for 3-4 days. The characterization and purity of molecules was assessed with liquid chromatography–mass spectroscopy (LC–MS). LC-MS data was obtained with an Agilent LC-MS equipped with Agilent 6530 Q-TOF with ESI source and Zorbax SB-C8 4.6 mm x 100 mm column for acidic conditions and a Zorbax Extend-C18 2.1 x 50 mm column for basic conditions. Mobile phases of each column were a gradient of water and acetonitrile containing 0.1% formic acid (for basic peptides) or 0.1% NH_4OH (for acidic peptides). Residual TFA adhering to positively charged PAs was then removed by treatment with HCl solution, and the remaining peptide residue was lyophilized. An Agilent 1200 series preparative reverse-phase high performance liquid chromatography (HPLC) system was used for the purification of molecules and was equipped with a Zorbax Extend-C18 21.2 x 150 mm column for basic conditions and a Zorbax SB-C8 21.2 x150 mm

column for acidic conditions. As the mobile phase of each column, a gradient of water and acetonitrile containing 0.1% TFA or 0.1% NH_4OH was used according to the charge of conditions.

In order to enable nanofibrous gel formation through charge neutralization, each of oppositely charged PAs was reconstituted in 0.25 M glucose solution prepared in ultrapure water and mixed at the molar ratio of 1:2 for the HM-PA / K-PA combination (resulting in a bioactive PA mixture) and 1:1 molar ratio for the E-PA / K-PA (resulting in a non-bioactive control PA mixture). Total charges of both mixtures were -1. The pH of peptide solutions was adjusted to 7.4 and peptide mixtures were sterilized with UV light for 1 h prior to use.

2.2.3. Physical and Mechanical Characterization of Self-Assembled Peptide Nanofiber Networks

2.2.3.1. Scanning Electron Microscopy (SEM)

Nanofiber networks formed by HM-PA / K-PA (1:2 molar ratio) and E-PA / K-PA (1:1 molar ratio) were inspected through SEM. Samples for SEM were prepared by incubating peptide nanofiber gels (1 wt %) with a final volume 60 µL for 20 min on silicon wafers. The peptide nanofiber gels were then dehydrated by sequential treatment with increasing concentrations of ethanol (20%, 40%, 60%, 80% v/v) for 2 min per wash and left in 100% absolute ethanol until drying in a critical point drier (Tousimis, Autosamdri-815B). Before the imaging process, samples were coated with 6 nm of Au/Pd layer and images were taken with a FEI Quanta 200 FEG scanning electron microscope under high vacuum with 5 keV beam energy.

2.2.3.2. Oscillatory Rheology

An Anton Paar Physica RM301 rheometer operating with a 25 mm parallel plate at 21 °C was used for oscillatory rheology measurements. In order to measure storage (G') and loss (G") moduli, HM-PA or control nanofiber gels (1 wt %) with total volume of 300 µL were loaded on the center of the lower plate and incubated for 15 min prior to measurement while upper plate was brought to a 0.5 mm gap position. While taking storage moduli (G') and loss moduli (G") measurements, angular frequency was adjusted from 100 to 0.1 rad/s, with a shear strain of 0.5%. The process was repeated 3 times for each peptide nanofiber gel and consecutive measurements were averaged for each sample.

2.2.3.3. Circular Dichroism (CD)

Secondary structures of HM-PA nanofiber or control nanofiber assemblies were examined by CD spectroscopy using a J-815 Jasco CD spectrophotometer at room temperature. Initially, PA stock solutions were prepared at 1 mM concentration and diluted to a concentration of 3.6×10^{-4} M for CD spectroscopy. Measurements were obtained 3 times in the range of 300 nm to 190 nm with 100 nm/min scanning speed, 1 nm bandwidth and 0.1 nm data pitch and 0.1 nm data interval, with digital integration time (1 DIT) as 1 s at standard sensitivity. Three consecutive measurements were averaged for each sample. The results were modified and shown as molar ellipticity.

2.2.4. *In vivo* Burn Model

All procedures performed in the present study were approved by The Animal Experiments Ethical Committee of Gazi University. *In vivo* experiments were carried out with 3-4 months old (20-30 g) male BALB/c mice. A total of 60 male mice were

randomly divided into 4 groups for HM-PA nanofiber treatment (n = 15), control nanofiber treatment (n = 15), sucrose solution treatment (n = 15) and 3M™ Tegaderm™ hydrogel treatment (n=15). Mice were maintained on *ad libitum* access to a standard laboratory diet in a 12-12 h light-dark cycle. Mice were anesthetized by intraperitoneal injection of ketamine hydrochloride (45 mg/kg) and xylazine hydrochloride (5 mg/kg). Under deep anesthesia, long hairs found on their dorsa were removed with a clipper and then shaved by a razor blade for complete hair removal. After the sterilization of underlying skin with povidone iodide, 3rd degree burns were generated with a custom made 200 g aluminum rod heated to 100 °C in a boiling water bath for 10 min. The tip of the aluminum rod was used as a template to generate 1 cm^2 wounds with square shapes on the posterior-dorsum of each mouse for 6 s. Within 30 min of burning, mice were resuscitated through intraperitoneal injection of saline using half-strength Parkland formula (4 mL/kg x percent body area). After 48 h, full thickness skin layers were removed from the wounds using a biopsy punch to generate 6 mm-diameter wounds. The debridement process was performed to accurately reflect the current medical standard for the treatment of burn injuries. The wounds were then treated with bioactive or non-bioactive peptide solutions, 0.25 M sucrose solution or 3M™ Tegaderm™ hydrogel. Lyophilized peptide masses were dissolved in 0.25 M sucrose solution to preserve osmotic balance. Gels were prepared by mixing oppositely charged PA molecules at a final concentration of 1 wt % immediately prior to application. 0.25 M sucrose solution was used as a negative control, while 3M™ Tegaderm™ hydrogel was used as positive control. Following the application of each treatment, wounds were covered with gauze dressing and impregnated with saline, and a long-term adhesive, air permeable, elastic and sterile bandage (OctaCare®) was placed over the wound to stabilize the position of

treatments. Gels (and sucrose solution) were re-applied and the wounds were re-dressed two days post-wounding. Mice were then individually caged and allowed to eat and drink *ad libitum* and routine controls were conducted throughout the study for infection and body weight loss. Animals were sacrificed at each experimental end point (day 0, day 7, day 14, day 21) and their tissues were extracted to continue with further analysis. Half of the tissue was used for histological analysis and the other half was used for RNA and protein analysis.

2.2.5. Wound Area Measurement

Wounds were photographed on days 7, 9, 12, 14, 16, 19 and 21 post wounding with a ruler. The scab areas on top of the wound were measured and calculated with Image J software (NIH, USA).

2.2.6. Histological Analysis

Half of the skin tissues of sacrificed mice were collected at days 7, 14 and 21, and fixed in 10% formalin. Following the fixation of extracts, samples were dehydrated in serially increasing concentrations of ethanol (70%-100%), embedded in paraffin and 5 µm skin sections were serially taken using a microtome. Tissue sections were incubated at 58 °C overnight and stained with hematoxylin and eosin (H&E), Masson's trichrome and picrosirius red with standard protocols after deparaffinization in xylene and rehydration in gradually decreasing concentrations of ethanol (%100-%70). All the quantifications from H&E and Massons' trichrome staining were performed using Image J. Images from these stainings were acquired using an upright microscope (Zeiss Axio Scope A1) at 5x and 10x magnifications, and then merged to observe whole skin tissue. Firstly, whole granulation area was traced and measured from wound edges and remaining muscle tissue at both sites. Wound closure was

measured at three different layers and their average was taken to best represent the extent of repair. The crust area was also traced and measured. Re-epithelization was quantified by measuring the remaining gap between left and right wound edges. Newly formed skin appendages were counted in the burned area and their density was calculated. Newly synthesized collagen was also quantified. Orientation of collagen fibers was analyzed using the Image J plug-in Orientation J. Scoring was also confirmed by researchers who were blind to the study design.

2.2.7. Immunohistochemical Staining

For immunohistological stainings, the tissue sections were deparaffinized in xylene and rehydrated in graded ethanol solutions and left in distilled water. Enzymatic antigen retrieval was performed with 0.1% pronase for 10 min at 35 °C or heat mediated antigen retrieval was performed with sodium citrate buffer (pH 6.0) using the guidelines provided by Abcam. Endogenous peroxidase activity was then inhibited with 3% hydrogen peroxide for 10 min at room temperature. Thereafter, normal goat serum was used to block non-specific binding sites by treating slides for 2 h at room temperature. Slides were incubated with anti-von Willebrand factor (1:400; ab6994, Abcam) overnight, followed by HRP conjugated goat anti-rabbit secondary antibody (1:500, Millipore (12-349)) on the next day. Antibody staining was followed by staining with 3,3'-diaminobenzidine (DAB) and counterstaining with hematoxylin. Mounting was performed with a xylene based mounting medium. Digital images of the granulation area were acquired using an up-right microscope (Zeiss Axio Scope A1) at 100x magnification and merged to count newly formed blood vessels. Quantifications were performed by ImageJ to calculate vessel density in each granulation field.

2.2.8. Protein and RNA Isolation from tissue

The simultaneous isolation of RNA and protein from burn wound samples was performed by using TRIzol reagent according to the manufacturer's protocol with minor adaptations and is briefly described below [157, 158]. Firstly, tissue was weighed and cut into small pieces with the help of a sterile surgical knife. Then, tissue pieces were smashed with liquid nitrogen until they became powder-like, and samples were homogenized with a power homogenizer with 1 mL of TRIzol reagent per 50-100 mg of tissue sample. The homogenate was incubated for 5 min to permit the complete dissociation of the nucleo-protein complex, mixed with chloroform (0.2 mL of chloroform per 1 mL of TRIzol reagent was used for initial homogenization) with vigorous shaking and centrifuged, which yielded a colorless top aqueous phase, an interphase, and an organic bottom phase. RNA was precipitated from aqueous phase by addition of isopropanol (0.5 mL of 100% isopropanol to aqueous phase per 1 mL of TRIzol reagent), mixed 15 times (up-down) and incubated at room temperature for 10 min. Then, the mixture was centrifuged to allow the formation of a gel-like RNA pellet, washed with 2 mL of 75% ethanol, air-dried for 5-10 min, dissolved in RNase-free water by pipetting and stored at -20 °C until use. DNA was precipitated from the interphase and organic phase by the addition of ethanol (0.3 mL of 100% ethanol per 1 mL TRIzol reagent used for initial homogenization) and centrifuged. Phenol-ethanol supernatant was removed and saved for protein precipitation by the addition of isopropanol (1.2 mL of isopropanol per 1 mL of TRIzol reagent was used for initial homogenization). The protein-isopropanol mixture was incubated overnight at -20 °C to allow the precipitation of proteins and centrifuged to pellet them. The protein pellet was washed with 2 mL of cold 0.3 M guanidine hydrochloride prepared in 95% ethanol 3 times with 20 min of incubation between each washing, and then washed

with ethanol at the last washing step. The protein pellet was left to air-dry for 5-10 min, dissolved with 10 M urea containing a protease inhibitor cocktail (Sigma) [158] and stored at -20 °C until use.

2.2.9. Quantitative Reverse Transcription Polymerase Chain Reaction

The gene expression profiles of angiogenesis inducing growth factors were evaluated by quantitative reverse transcription polymerase chain reaction (qRT-PCR) analysis. Yield and purity of extracted RNA were assessed using the Nanodrop 2000 system (Thermo Scientific). Primer sequences for growth factors were selected according to their suitability by using PREMIER Bio-soft software (Table 1). Reaction efficiencies for each primer set were evaluated with standard curves using at least 5-fold serial dilutions of total RNA after the optimization of their annealing temperatures. SuperScript III Platinum SYBR Green One-Step qRT-PCR kit (Invitrogen) was used for cDNA synthesis and PCR according to the manufacturers' instructions. Reaction conditions were briefly as follows: 55 °C for 5 min, 95 °C for 5 min, 40 cycles of 95 °C for 15 s, T_m (60 °C, 60 °C and 58 °C for VEGF, bFGF, GAPDH, respectively) for 30 s, and 40 °C for 1 min, which was followed by melting curve analysis to confirm product specificity after each reaction. VEGF and bFGF gene expression profiles were analyzed at days 7, 14 and 21. For the analysis of expression, primary gene expression data were normalized to the expression level of GAPDH in each run, which served as the internal control gene. Each group was then normalized to the expression levels of sucrose solution treated groups, which served as a negative control. mRNA levels were calculated according to the comparative Ct method with effciency correction for each target gene.

Table 1. Primer sequences used for qRT-PCR expression analysis

Gene	Primer Sequences: Forward / Reverse	Melting Temperature
FGF-2 (bFGF)	5'- GAGAAGAGCGACCCACACG - 3'	60 °C
FGF-2 (bFGF)	5'- GGCACACACTCCCTTGATAGA - 3'	
$VEGF_{165}$	5'- CTGTAACGATGAAGCCCTGGAG - 3'	60 °C
$VEGF_{165}$	5'- TGGTGAGGTTTGATCCGCAT - 3'	
GAPDH	5'- GTCAAGCTCATTTCCTGGTATG - 3'	58 °C
GAPDH	5'- CTCTCTTGCTCAGTGTCCTTG - 3'	

2.2.10. Western Blot Analysis

After sacrificing the animals, half of the tissue samples collected from animals were taken into microcentrifuge tubes and immediately frozen with liquid nitrogen to further characterize the expression levels of proteins at days 7, 14 and 21 of the burn wound healing process. Total protein in each sample was solubilized with 0.3 mL of 10 M urea and quantified with BCA assays (Thermo Scientific) using a 1:50 dilution rate to eliminate the absorbance coming from urea itself and to accurately quantify the protein stock concentration. Equal amounts of proteins (70 ng, 20 μL) were resolved on 10% SDS-PAGE under denaturing and reducing conditions and transferred to polyvinylidene difluoride (PVDF) membranes (Thermo Scientific). Membranes were blocked with 5% non-fat milk in TBS-T for 1 h at room temperature and then incubated with primary antibody at 4 °C overnight. Anti-VEGF and anti-α-SMA antibodies were purchased from Millipore (ABS82, (1:750) and 04-1094, (1:1000),

respectively). Anti-GAPDH antibody was used as internal control and purchased from Millipore (MAB374 (1:500)). After washing in TBS-T, membranes were incubated with a corresponding HRP-coupled secondary antibody for 1 h at room temperature. Anti-rabbit IgG-HRP (purchased from Abcam) and anti-mouse IgG-HRP (purchased from Millipore, 12-349) were used at dilutions of 1:2000 and 1:1000, respectively. Signals were visualized using enhanced chemiluminescence analysis on a ChemiDoc™ Imaging System with Image Lab™ Software (Bio-Rad). Protein concentrations were quantified with ImageJ software and intensities of VEGF and α-SMA were normalized to GAPDH.

2.2.11. Statistical Analysis

Statistical analyses were performed by using GraphPad Prism 6 software. One way ANOVA with Tukey's post-tests or two way ANOVA with Bonferroni post-tests was employed to determine the statistical differences between groups, where appropriate. Error bars indicate the standard error of the mean. The level of significance was set at $p<0.05$.

2.3. Results

2.3.1. Synthesis and characterization of PA molecules

Heparin-mimetic (HM-PA), negatively charged E-PA and positively charged K-PA molecules were synthesized by solid phase peptide synthesis method, purified by preparative HPLC and their molecular weights were confirmed by mass spectrometry analysis prior to their use (Figure 10-12). The structure of the HM-PA molecule was designed to mimic that of heparin through the presentation of sulfonate, hydroxyl and carboxylate groups, while E-PA was used as a non-bioactive control peptide lacking reactive groups on its amino acid side chains (Figure 9a) [118]. When mixed with the

positively-charged K-PA at neutral pH, both peptide molecules self-assembled into fibrous networks that closely resemble the structure of the extracellular matrix (Figure 9 d, e) and feature an abundance of β-sheets, while the individual PA molecules did not self-assemble in the absence of a charge-neutralizing agent and exhibited random coil structures (Figure 9 b). Storage and loss moduli of both bioactive and non-bioactive peptide scaffolds were comparable to those of the commercial wound dressing 3M™ Tegaderm™ (Figure 9g). A representative image of PA nanofiber gels is shown in Figure 9f.

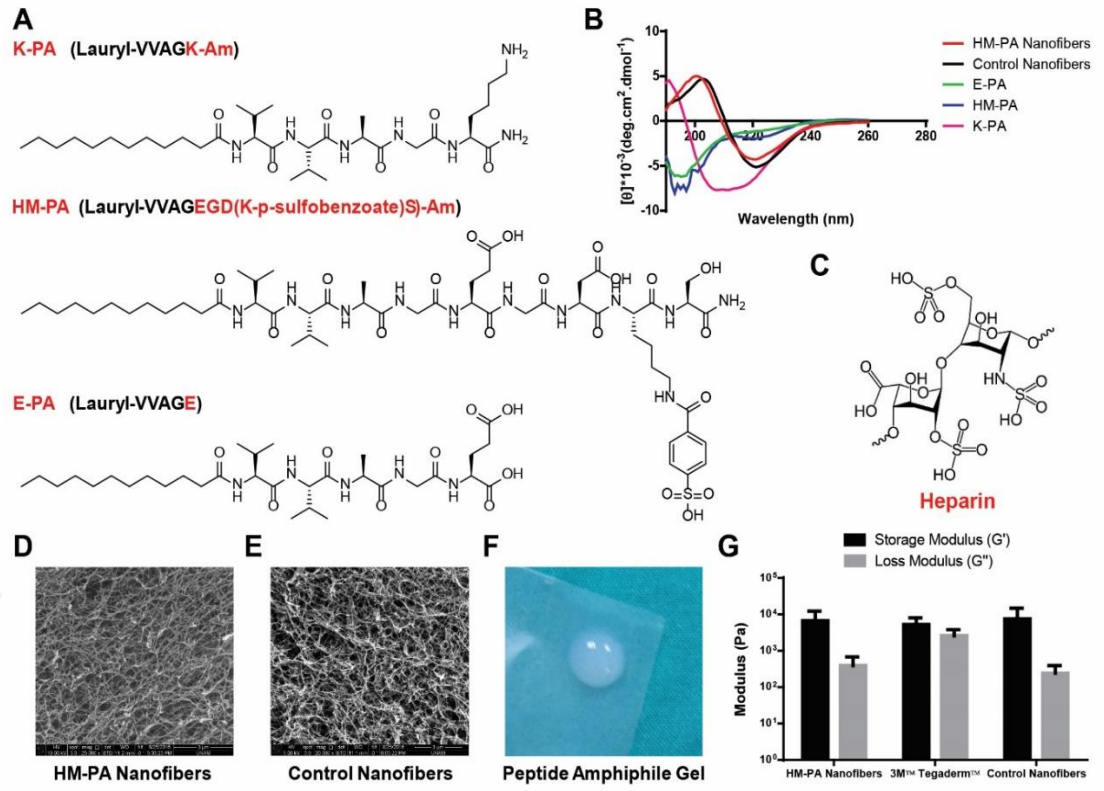

Figure 9. Chemical structures of K-PA, HM-PA and E-PA. (A) Characterization of peptide amphiphile molecules and their nanofibers with circular dichroism. (B) Structure of Heparin. (C) Characterization of peptide nanofibers at pH 7.4 by using SEM. (D,E) General appearance of peptide nanofiber gels (F). Rheology measurements of scaffolds (G). Scale bars are 5 µm.

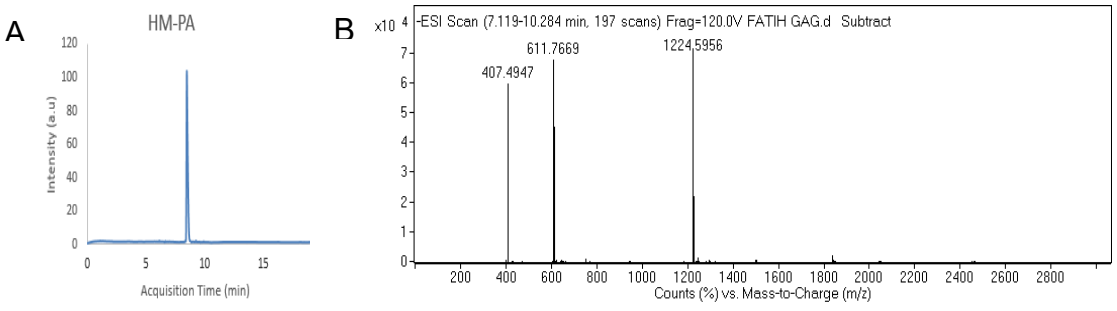

Figure 10. (A) RP-HPLC chromatogram of HM-PA , the change of response units with respect to time at 220 nm. (B) Mass spectrometry of HM-PA. $[M-H]^-$ (calculated): 1225.59, $[M-H]^-$ (observed): 1224.59, $[M-2H]^{-2}/2$ (calculated): 611.79, $[M-2H]^{-2}/2$ (observed): 611.76 $[M-3H]^{-3}/3$ (calculated): 407.53, $[M-3H]^{-3}/3$ (observed): 407.49.

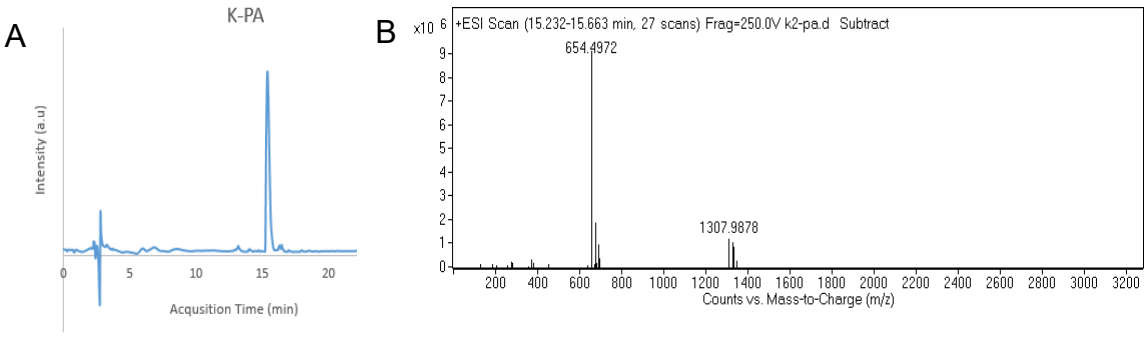

Figure 11. (A) RP-HPLC chromatogram of K-PA , the change of response units with respect to time at 220 nm. (B) Mass spectrometry of K-PA. $[M+H]^+$ (calculated):653.48, $[M+H]^+$ (observed): 654.49, $[2M+H]^+$(calculated): 1307.96 $[2M+H]^+$ (observed): 1307.98.

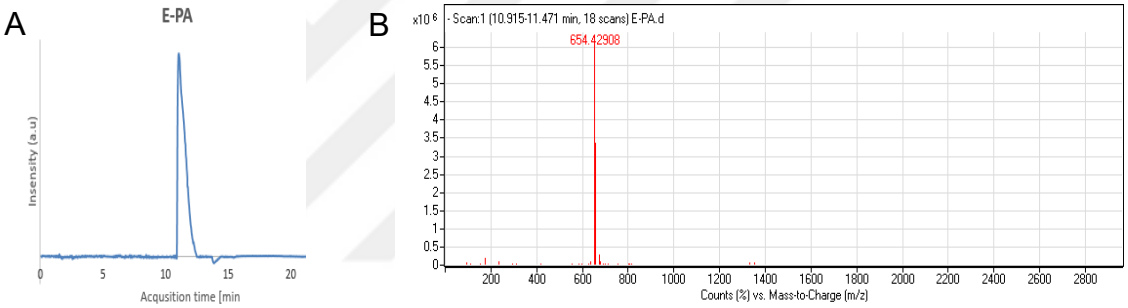

Figure 12. (A) RP-HPLC chromatogram of E-PA , the change of response units with respect to time at 220 nm. (B) Mass spectrometry of E-PA. $[M-H]^-$ (calculated): 655.42, $[M-H]^-$ (observed): 654.42.

2.3.2. Gel treatment and dorsal burn injury model

Full-thickness dorsal burn wounds were created following a protocol modified from Sun *et al.* (Figure 13) [159]. Briefly, 1 cm^2 aluminum plaques were heated to 100 °C in boiling water for 10 min and applied to the dorsum of anesthetized mice for ~6 s to inflict third-degree burn injuries. These injuries were allowed to develop for 2 days, and a 6 mm skin punch was used to remove necrotic tissue at full-thickness depth from the center of the burn wound (Figure 13).

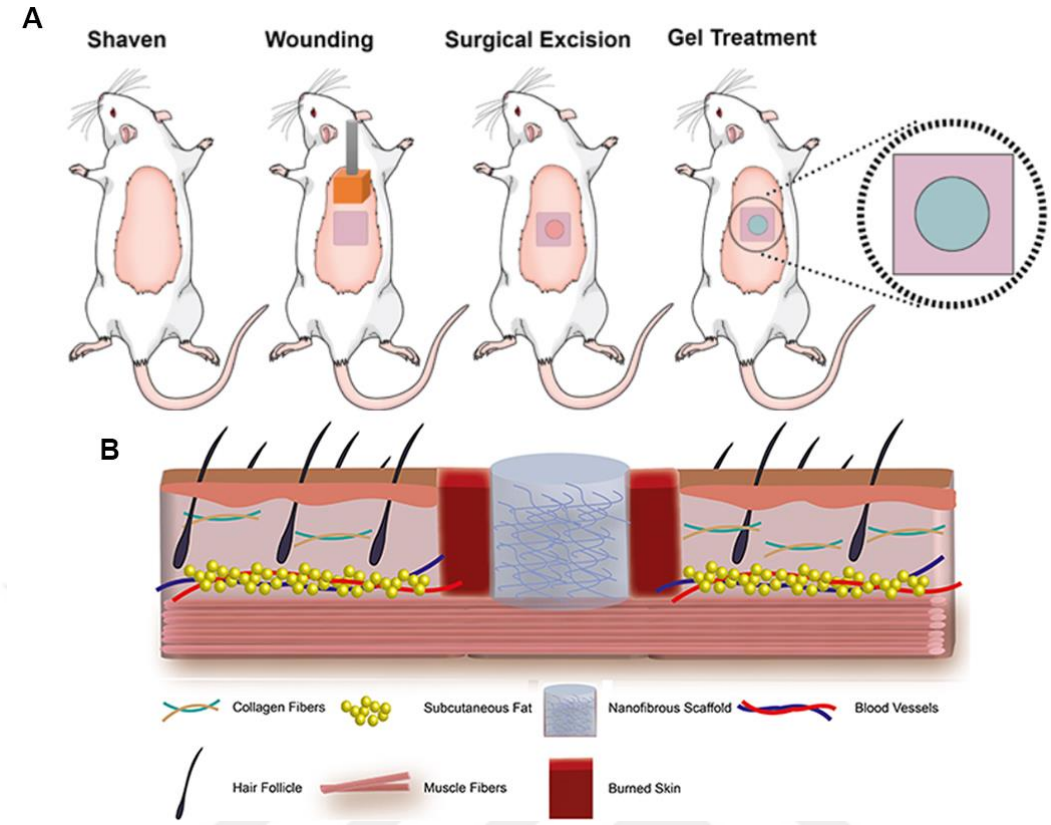

Figure 13. Schematic representation of full-thickness burn wound model. (a) A pre-heated aluminum plaque was applied to the shaved dorsum of the anesthetized mouse; followed by the removal of the injured skin and the application of the hydrogel. (b) A schematic of the hydrogel-implanted wound site. Schematic representations of the burn model were prepared using Mind the Graph software.

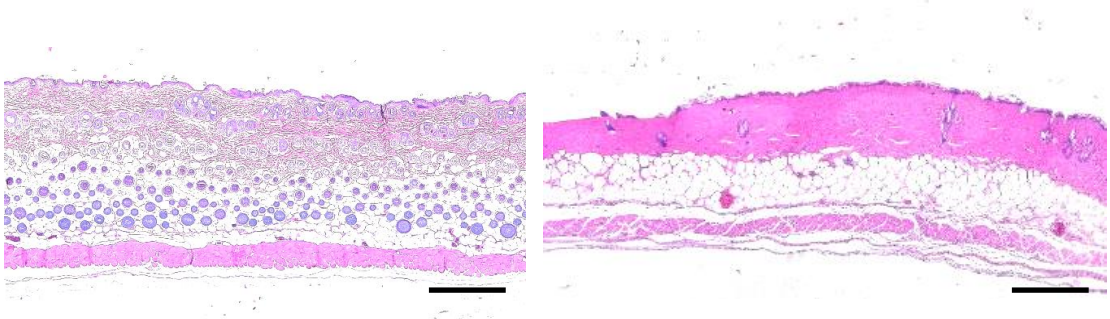

Figure 14. Comparison of normal mouse skin with full-thickness burned mouse skin. Scale bars are 500 µm.

The defect left by the removed tissue was then covered with either a peptide nanofiber hydrogel (HM-PA / K-PA or E-PA / K-PA), the commercial wound filler 3M™ Tegaderm™, or 0.25 M sucrose solution. Wounds were visually monitored daily (Figure 15 a) and 5 animals from each group were sacrificed for histological analysis at days 7, 14 and 21. Animal weights were also controlled throughout the study duration to eliminate the possibility of excessive weight loss due to trauma (Figure 16). Wound recovery was observed to be enhanced in wounds treated with HM-PA peptide nanofibers, with significantly smaller wound areas at days 12, 14 and 16 (Figure 15 b). In contrast, neither the non-bioactive peptide mixture nor the 3M™ Tegaderm™ filling enhanced wound closure compared to the negative control (0.25 mM sucrose) within the first 16 days of recovery, although wound closure was complete in all groups at day 21. In addition, HM-PA peptide nanofiber-treated wounds exhibited a dense fur covering on top of the closed wound (which was partially shaved prior to wound imaging), while 3M™ Tegaderm™ - and sucrose-treated groups had limited fur growth (Figure 15 a).

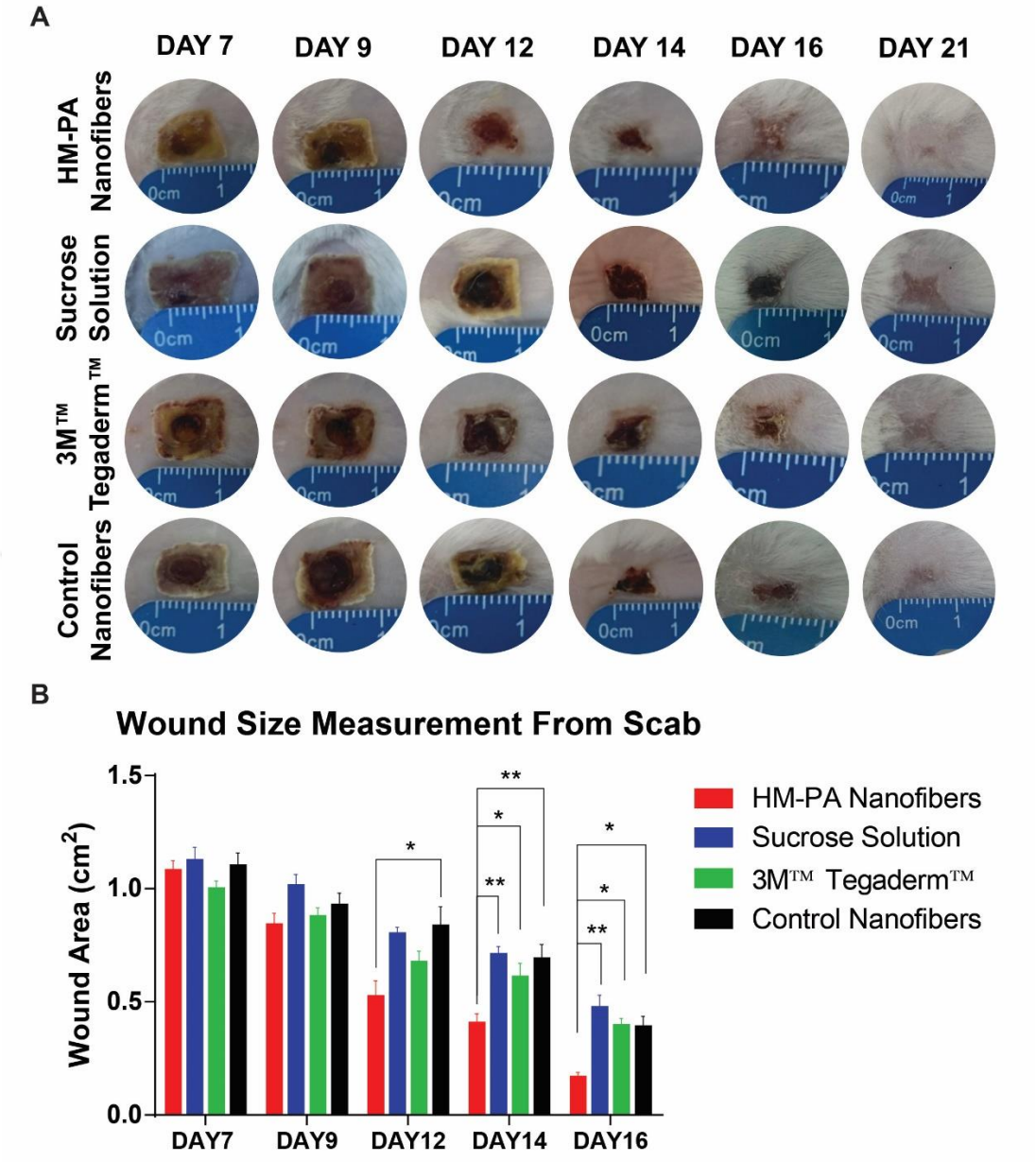

Figure 15. Representative images of burn wounds after gel application at days 7, 9, 12, 14, 16 and 21 (A). Quantification of wound areas treated with HM-PA peptide nanofibers, sucrose solution, 3M™ Tegaderm™ and control nanofibers at days 7, 9, 14, and 16 (B). One-way ANOVA (Bonferroni's multiple comparisons test) was used for statistical analysis. Error bars represent standard error of mean.

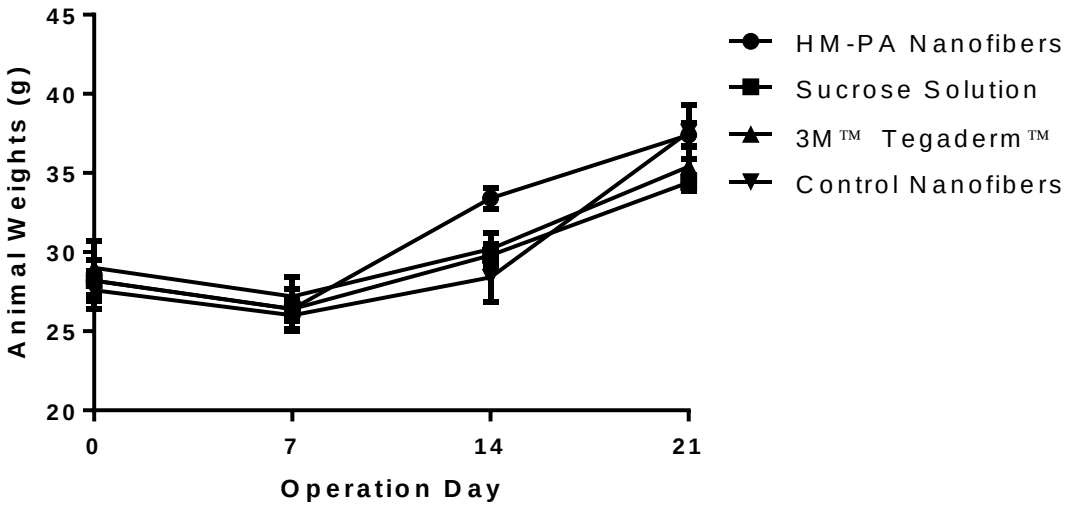

Figure 16. Animal weights throughout the study.

2.3.3. Histological analysis

The effective recovery of burn wounds depends not only on the closure of the wound itself, but also on the replacement of damaged extracellular matrix with freshly deposited collagen, the removal of local debris from the wound site and the formation of new skin appendages [160]. As such, skin sections taken at 7, 14 and 21 days following peptide nanofiber gel, 3M™ Tegaderm™ or sucrose application were stained with H&E and Masson's trichrome to observe the local morphology of the site of injury (Figure 17 a). Granulation, re-epithelialization, crust formation, wound contraction and skin appendage development were also monitored to determine the extent of functional wound recovery. The gradual decrease of granulation area is one of the main hallmarks of skin wound recovery and occurs through the contractile activity of myofibroblasts. HM-PA peptide nanofiber gel treatment was found to result in significantly smaller granulation tissue areas at day 7, suggesting that the heparin-mimetic hydrogel enhanced fibroblast recruitment and/or the differentiation of local fibroblasts into myofibroblasts (Figure 17 b). A similar trend was also observed in average wound distance results, which also strongly depend on myofibroblast activity and suggest that wound contraction was enhanced by bioactive peptide nanofiber gel treatment at day 7 (Figure 17 c).

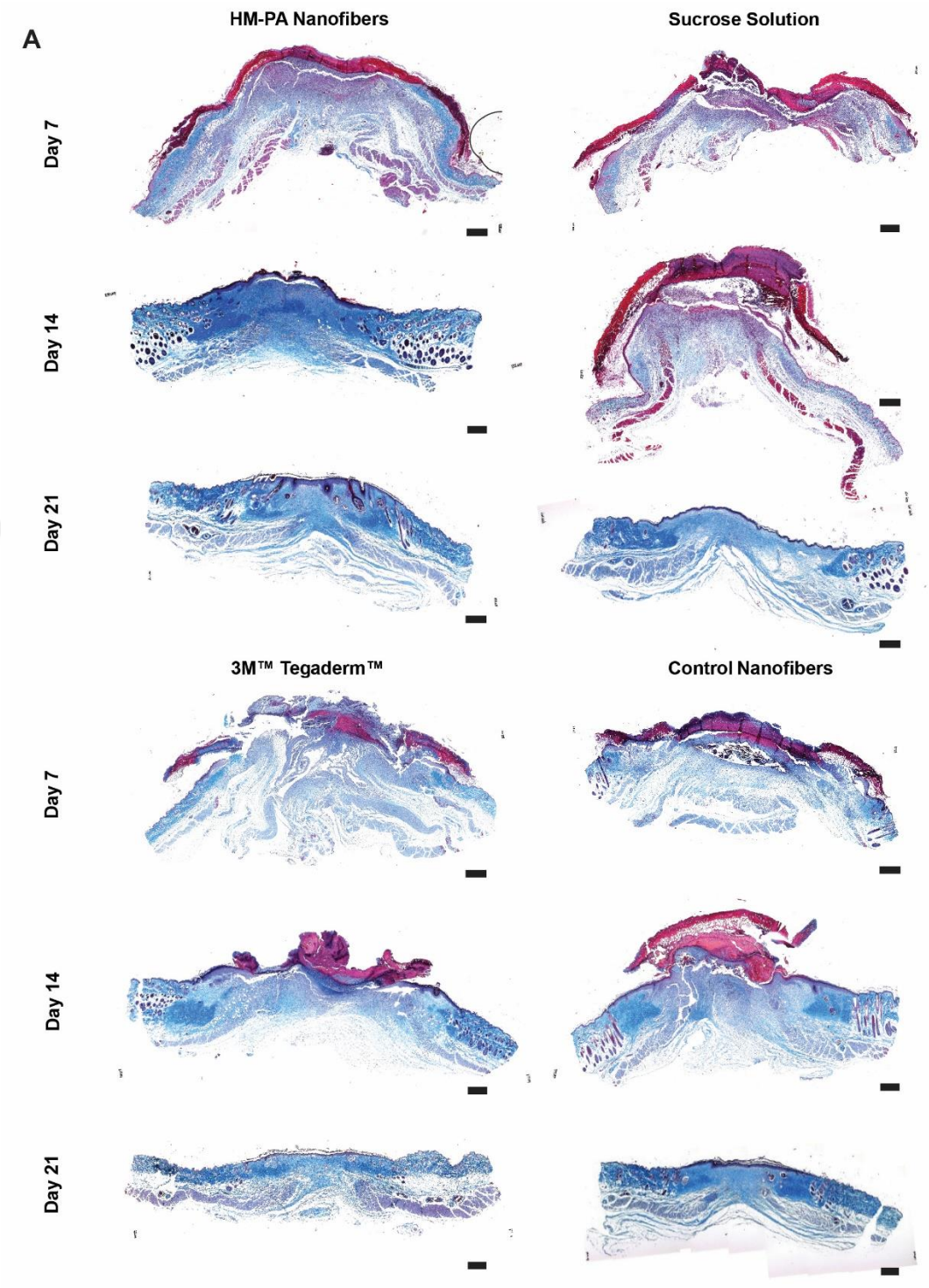
A
HM-PA Nanofibers
Sucrose Solution
Day 7
Day 14
Day 21
3M™ Tegaderm™
Control Nanofibers
Day 7
Day 14
Day 21

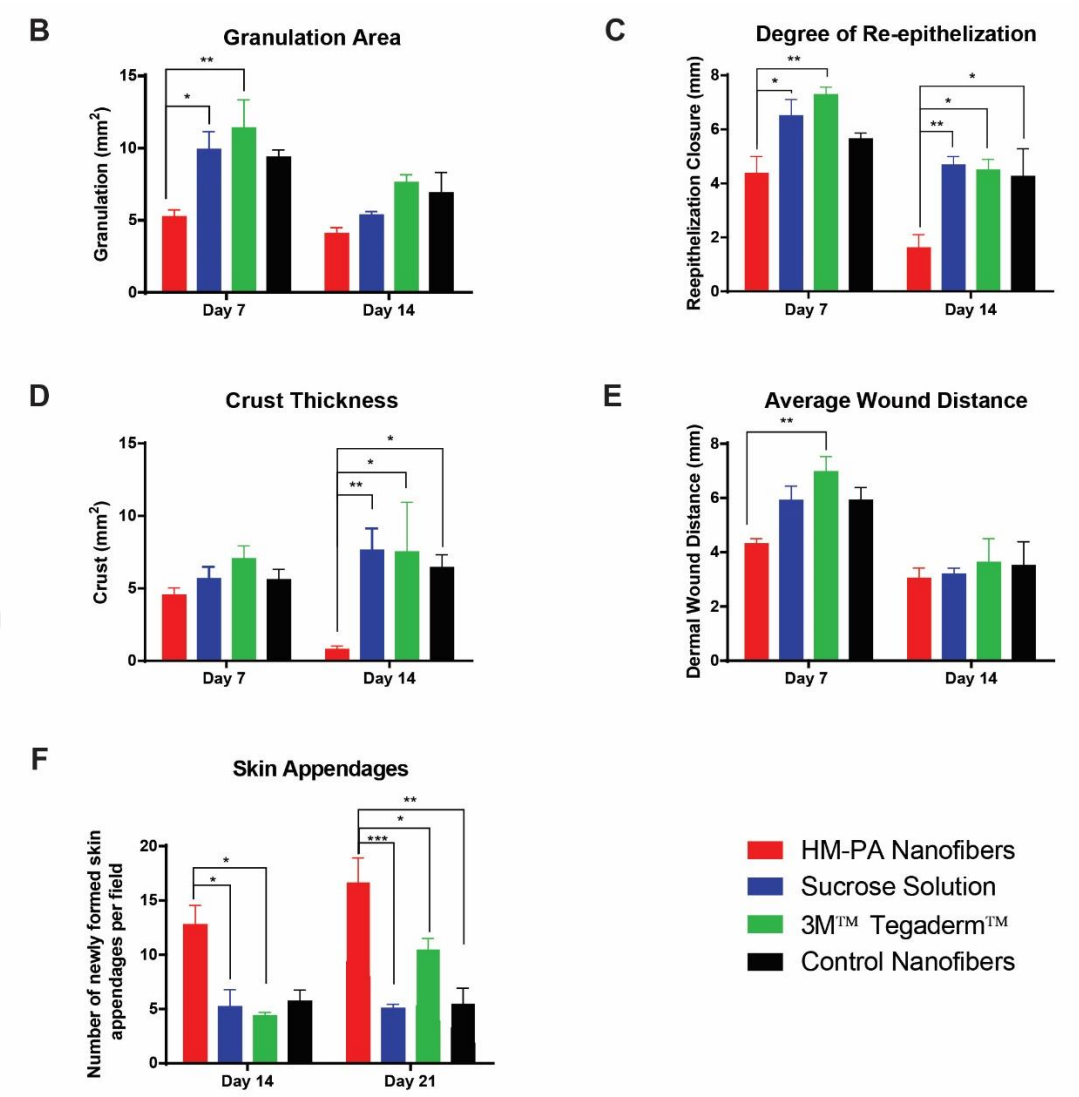

Figure 17. Masson's Trichrome staining of HM-PA nanofiber, sucrose solution, 3M™ Tegaderm™ and control nanofiber application at days 7, 14 and 21 (A). Scale bars are 500 µm. Quantitative analysis of granulation tissue (B), re-epithelization (C), crust area (D), wound distance (E) and skin appendages (F) of burn wounds at days 7, 14 and 21. One-way ANOVA (Bonferroni's multiple comparisons test) was used for statistical analysis, *p< 0.05. Error bars represent standard error of mean.

In addition to the physical contraction of the site of injury, wound recovery also depends on the local remodeling of the extracellular matrix for the removal of local

debris and deposition of new matrix proteins. While HM-PA peptide nanofiber treatment had a significant impact on wound closure at the earlier stages of the recovery process, its effects on matrix remodeling were longer-lasting. In particular, bioactive peptide nanofiber treated wounds had significantly shorter gaps in newly formed epithelial tissue at both day 7 and day 14, exhibiting mean epithelial gap distances of 4.4 and 1.6 mm at these time periods (compared to 6.5 and 4.7 mm for sucrose and 7.3 and 4.5 mm for 3M™ Tegaderm™) (Figure 17 d). In addition, the successful remodeling of the wound site following HM-PA peptide nanofiber treatment was also associated with the rapid degradation of the wound crust, which was 9.7- and 9.5-folds thinner than the sucrose and 3M™ Tegaderm™-treated groups at day 14 (Figure 17 e). Furthermore, bioactive peptide nanofiber-treated wounds had 16.67 ± 5.03 skin appendages per granulation area at day 21, compared to 5.08 ± 0.82 and 10.49 ± 1.73 in sucrose and 3M™ Tegaderm™-treated wounds, suggesting that extracellular matrix remodeling was mostly complete by this time period and that the remodeled skin was well into the process of being repopulated by skin appendages (Figure 17 f).

2.3.4. Modulation of angiogenesis by bioactive peptide nanofiber scaffolds

A complex set of signaling interactions is required for the recruitment, differentiation and survival of the cells that drive the wound recovery process. The formation of new blood vessels is a major aspect of these interactions, and angiogenesis-promoting scaffolds can effectively support wound healing by ensuring the transport of oxygen, nutrients and signaling molecules to cells at the site of injury. As such, the ability of the HM-PA peptide nanofiber hydrogels to support neovascularization was tested by anti-von Willebrand factor staining and the quantification of newly formed blood vessels at the wound site. Bioactive peptide nanofiber treatment was observed to

greatly enhance angiogenesis at the wound site at day 7, with a smaller (but statistically significant compared to non-bioactive peptide nanofiber and 3M™ Tegaderm™) increase at day 14, which is consistent with the early induction of angiogenesis in the presence of the bioactive peptide nanofibers (Figure 18). However, compared to control nanofiber and 3M™ Tegaderm™, blood vessel density was significantly lower in HM-PA peptide nanofiber-treated wounds at day 21, which suggests that wound recovery was complete at this time period and that most of the blood vessels present at the former wound site had been resorbed (Figure 18 b).

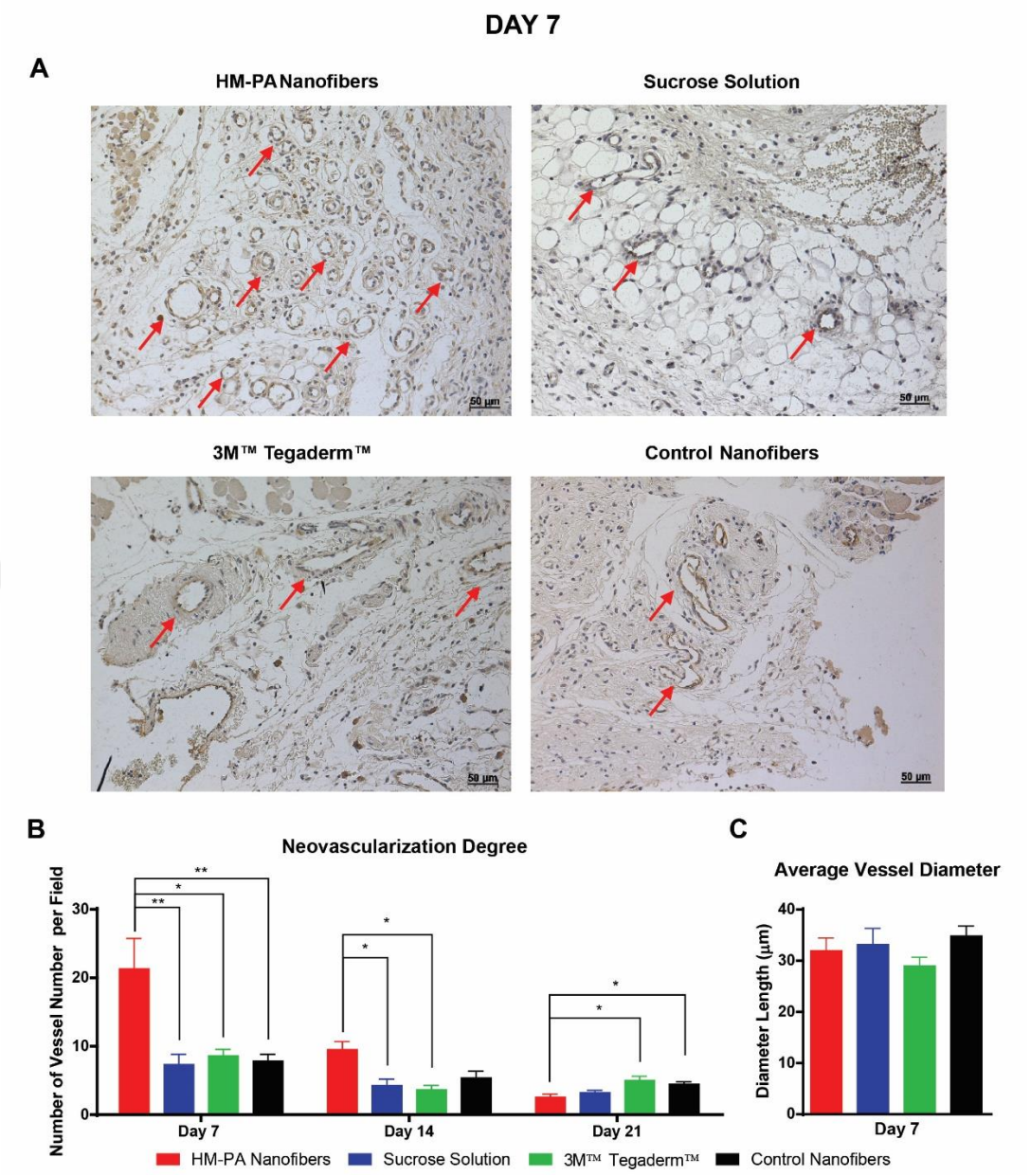

Figure 18. Staining of blood vessels by anti-VWF and quantification of blood vessels at days 7, 14 and 21 (A,B). Quantification of average vessel diameter at day 7 (C). One-way ANOVA (Bonferroni's multiple comparisons test) was used for statistical analysis. Arrows indicates the newly formed blood vessels. Errors bars represent standard error of mean. Scale bars are 50 µm.

The qRT-PCR analysis of VEGF and FGF-2 further supported these results, as the considerable increase in angiogenic factor expression at day 7 was observed to

decrease at days 14 and 21 in the HM-PA peptide nanofiber-treated group (Figure 19). Expression of VEGF was further confirmed by Western analysis at day 7 at protein level. Likewise, the protein-level expression of α-SMA was significantly enhanced at day 7 in the HM-PA peptide nanofiber-treated group compared to control peptide nanofiber gel and sucrose solution, which may indicate the early differentiation of fibroblasts into myofibroblasts in the presence of the bioactive peptide nanofiber hydrogel.

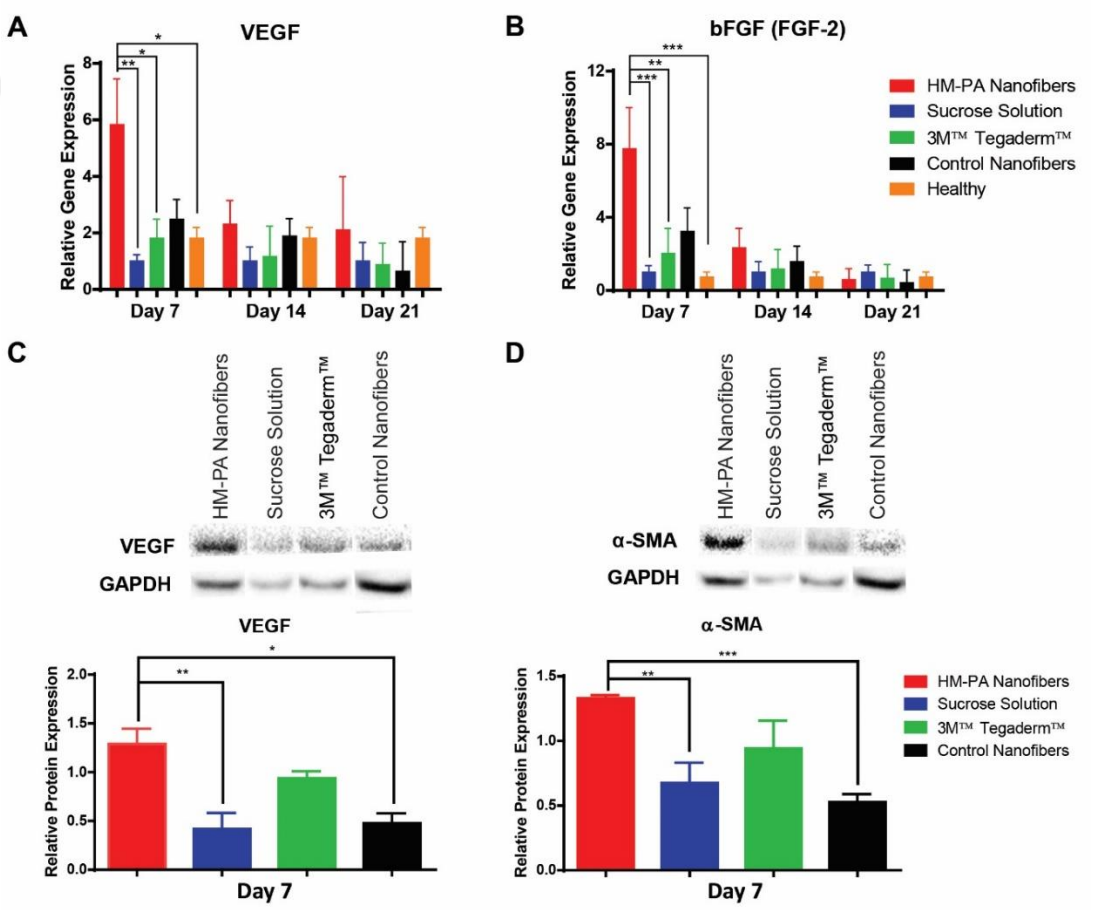

Figure 19. Protein and mRNA levels of genes associated with angiogenesis and wound repair at the burn wound site at days 7, 14 and 21. qRT-PCR analyses were performed for VEGF and bFGF (A, B), while Western blot analyses were performed for VEGF and -SMA (C, D). Statistical analysis was performed with one-

way ANOVA and Bonferroni's multiple comparisons test. Error bars represent standard error of mean.

2.3.5. Collagen orientation

The ability of bioactive and non-bioactive peptide nanofiber scaffolds and 3M™ Tegaderm™ to facilitate the deposition of well-crosslinked collagen fibers was investigated through the picrosirius red staining of skin sections at day 21 (Figure 20 a). In healthy skin, picrosirius red dye stains in distinctive bands due to the presence of hair follicles, sebaceous and sweat glands, and a highly organized collagen structure. In contrast, the wound area is characterized by uniform staining due to the disruption of the collagen network, and the restoration of the crosslinked collagen matrix is indicative of wound recovery. Accordingly, a highly homologous picrosirius red staining was observed in non-bioactive peptide nanofiber, 3M™ Tegaderm™ and sucrose-treated burn injuries, suggesting that collagen crosslinking is incomplete even at day 21 for these groups. However, a heterogeneous pattern of staining was observed in the HM-PA peptide nanofiber-treated wounds, which was consistent with an advanced state of recovery and the restoration of the regular architecture of skin. The orientation of collagen fibers were also quantified through the OrientationJ plugin of ImageJ software, and bioactive hydrogel-treated wounds were observed to exhibit two distinctive alignment directions, which is similar to healthy skin and indicative of crosslinking (Figure 20 b-c). Non-bioactive peptide nanofiber, 3M™ Tegaderm™ and sucrose-treated wounds, however, exhibited fiber orientation in only a single direction, suggesting that collagen crosslinking was not yet complete.

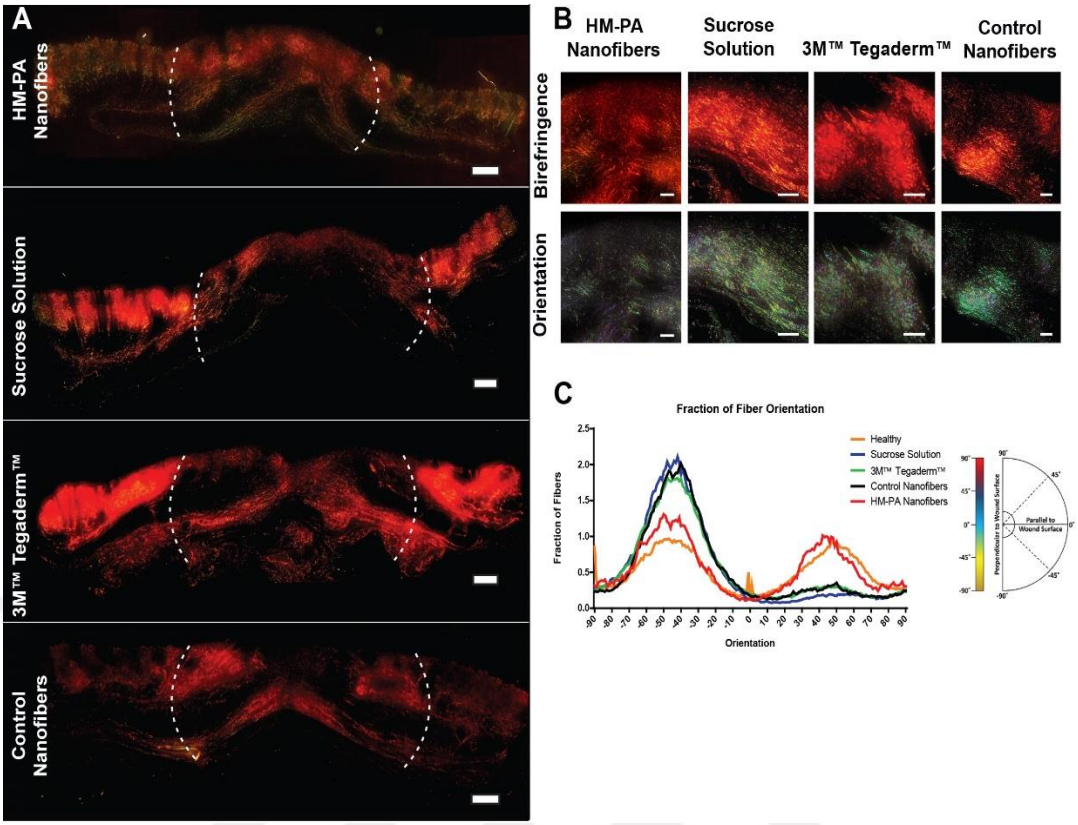

Figure 20. Fiber directionality resembles healthy tissue in HM-PA peptide nanofiber-treated burn wounds. Picrosirius red staining was performed to visualize collagen fiber orientation. Wound areas analyzed are highlighted with dashed lines (A, B). Healthy and HM-PA peptide nanofiber-treated fibers were distributed evenly between -50° and +50° orientations, while sucrose, 3M™ Tegaderm™- and control nanofiber-treated wounds exhibited collagen orientation only in the -50° direction (C).

2.4. Discussion

Severe burn wounds are characterized by a strong local immune response, higher metabolic rates at the site of injury, increased cortisol and cytokine levels, ingress of fluid from extracellular space to the wound site and limited transport of oxygen and nutrients, which result in the gradual necrosis of affected tissue [161]. Consequently, the effective repair of burn wounds requires the modulation of metabolic, immune, homeostatic and angiogenic responses. Heparin and heparan sulfate are

glycosaminoglycans that are abundantly expressed at the burn injury site and assist in the early wound healing process by preventing coagulation, activating a range of pro- and anti-inflammatory pathways and binding to growth factors such as VEGF, FGF, HGF and TGF-β that stimulate the proliferation of fibroblasts, muscle cells, epithelial cells and endothelial cells [162]. However, heparin is rapidly degraded in biological environments and, due to its animal origin, poses a risk of zoonotic contamination, which has stimulated the development of more advanced delivery systems for replicating its effects on tissues [163]. Hydrogel scaffolds are especially useful for this purpose, as their similarities to the extracellular matrix, ease of modification, ability to constantly hydrate the site of injury and potential co-delivery with cytokines, antibiotics, growth factors and/or stem cells are all highly relevant properties for the treatment of burn wounds [164].

The HM-PA peptide nanofibers mimic the activity of heparin and form a biocompatible gel at neutral pH. The HM-PA peptide nanofibers were previously shown to bind growth factors, enhance osteo-chondrogenic differentiation, improve the success of pancreatic islet transplantation and stimulate the repair of normal and diabetic wound injuries [13, 165-167]. Our present observations suggest that the growth factor-binding, water-retaining and glycosaminoglycan-mimicking features of HM-PA peptide nanofibers are also effective for stimulating the repair of full-thickness burn injuries. In particular, HM-PA peptide nanofiber-treated wounds had higher skin appendage formation, wound closure and re-epithelialization rates, as well as lower granulation tissue areas and thinner crust formation, at days 7 and 14 of the recovery process, which is consistent with the prominent roles played by heparin during early wound healing. While wound closure was mostly complete in all groups at day 21, the bioactive peptide nanofiber-treated group nevertheless exhibited enhanced fur

growth and a lack of scar tissue formation at later stages of recovery, and presented a greater amount of collagen remodeling in Masson's trichrome staining.

Angiogenesis is another aspect of wound healing and plays an especially important role in burn injuries due to the anoxic and nutrient-poor environment that characterizes these wounds [164]. However, blood vessels are typically resorbed following the completion of the healing process, and excessive angiogenesis at later stages of wound healing is also detrimental for the functionality of the repaired tissue, potentially contributing to the development of hypertrophic scars [168]. Consequently, a balance between angiogenic and anti-angiogenic responses is necessary for wound recovery, and the HM-PA peptide nanofibers are able to answer this need by mediating the required transition between the production and resorption of blood vessels. Anti-von Willebrand factor staining results suggest that, compared to sucrose and 3M™ Tegaderm™ treatment, neovascularization was heavily enhanced on day 7, slightly enhanced on day 14 and slightly impaired on day 21 in response to heparin-mimetic peptide nanofibers. VEGF, the main angiogenic factor in wound healing, was also strongly expressed at the HM-PA peptide nanofiber-treated wound site at day 7, while declining sharply at days 14 and 21. As HM-PA peptide nanofibers have previously been shown to specifically interact with $VEGF_{165}$ through its heparin-binding domain [13], it is likely that their presence enhances angiogenesis by retaining endogenously produced VEGF at the site of injury. The HM-PA peptide nanofibers also exhibit an affinity for the endothelial cell-stimulating factor FGF-2, of which expression was elevated following bioactive gel treatment.

Following injury, the collagen matrix at the wound site is completely denatured, leaving a disordered and necrosis-promoting extracellular environment. During the wound repair process, the cellular debris at the wound site is removed by

inflammatory cells, and a new, well-crosslinked collagen matrix is deposited by local and recruited fibroblasts. Collagen alignment can therefore be used as a measure of the wound healing progress, as healthy extracellular matrix is characterized by two axes of collagen fibers that intersect to create a basket-woven appearance, while the old, dysfunctional extracellular matrix exhibits only a single collagen axis [169]. In sucrose and 3M™ Tegaderm™-treated wounds, orientation analysis showed that collagen fibers were arranged in only a single axis, while healthy and HM-PA peptide nanofiber-treated tissues were characterized by the deposition of collagen in two axes of orientation. This enhancement of collagen crosslinking was also supported by the early expression of α-SMA, which is responsible for fibroblast activation, wound contraction and extracellular matrix remodeling. In addition, sucrose- and 3M™ Tegaderm™-treated samples exhibited some "gaps" without picrosirius red staining, suggesting that collagen deposition was incomplete in these samples, while the entire dermal layer was stained extensively with picrosirius red for healthy and HM-PA peptide nanofiber-treated samples.

2.5. Conclusions

In summary, we demonstrated that the heparin-mimetic peptide nanofibers are able to support the repair of full-thickness burn injuries by mediating wound contraction and re-epithelialization, preventing scar formation, and stimulating the development of skin appendages. In addition, enhanced wound recovery in the heparin-mimetic peptide nanofiber-treated group was found to be associated with the induction of neovascularization and the deposition of an extensively crosslinked collagen matrix. It is especially notable that the commercial wound filling 3M™ Tegaderm™ was significantly less effective in many of these aspects. The burn injury and treatment model used in the present study closely resembles the standard of care for burn

wounds, which entails the removal of necrotic tissue and the implantation of autografts and/or collagen-based scaffolds. As such, the HM-PA peptide nanofiber system can easily be adapted to clinical settings for moderate burn injuries that do not necessitate autograft treatment.

CHAPTER 3

CONCLUSIONS AND FUTURE DIRECTIONS

In this thesis, I have described the design and synthesis of a peptide amphiphile system that is able to enhance the repair of burn injuries in the mouse model. In particular, the HM-PA scaffold was able to prevent post-injury necrosis, increase cellular viability and recruitment, promote collagen deposition and crosslinking, and enhance angiogenesis, re-epithelialization and skin appendage formation compared to epitope-free peptide scaffolds and the commercial wound dressing 3M™ Tegaderm™. Positive effects were observed at all stages of the wound healing process, with rapid wound closure as a result of early proliferation and angiogenesis, and decreased scar formation due to enhanced collagen deposition at later days of recovery. The ability of HM-PA to stimulate angiogenesis during the early stages of recovery is especially crucial for its effectiveness, as blood vessel formation is a major requisite of healthy tissue repair. In contrast to the bioactive peptide system, the non-bioactive scaffold did not exhibit comparable effects despite similar physical and mechanical properties, suggesting that the heparin-binding and growth factor-retaining abilities of HM-PA were necessary for promoting wound healing in full-thickness burn wounds.

Peptide nanofibers are a promising means of enhancing the natural signaling pathways responsible for regulating cell and tissue repair. Their hydrogel structure, variable bioactive groups, ease of preparation, low batch-to-batch variance, and slow release capacity all contribute to their effectiveness in facilitating tissue recovery in a broad range of injury and disease models. However, there is a dearth of tissue engineering studies that explore the full potential of peptide amphiphiles in clinical settings, and few pharmacological companies include peptide scaffolds and similar materials in their portfolio. Consequently, comprehensive material characterization studies are necessary to demonstrate the safety and efficiency of peptide hydrogel-

based treatment systems in human patients. In the context of the present study, future efforts may focus towards developing the HM-PA scaffold for practical applications, potentially by using a broader range of injury models of varying severity, location, and prognosis.

REFERENCES

1. Shupp, J. W.; Nasabzadeh, T. J.; Rosenthal, D. S.; Jordan, M. H.; Fidler, P.; Jeng, J. C., A review of the local pathophysiologic bases of burn wound progression. *J Burn Care Res* **2010,** *31* (6), 849-73.

2. Rose, J. K.; Barrow, R. E.; Desai, M. H.; Herndon, D. N., Advances in burn care. *Adv Surg* **1996,** *30*, 71-95.

3. Lister, T.; Wright, P. A.; Chappell, P. H., Optical properties of human skin. *J Biomed Opt* **2012,** *17* (9), 90901-1. DOI: 10.1117/1.JBO.17.9.090901.

4. Huang, H. C.; Chang, T. M., Ceramide 1 and ceramide 3 act synergistically on skin hydration and the transepidermal water loss of sodium lauryl sulfate-irritated skin. *Int J Dermatol* **2008,** *47* (8), 812-9. DOI: 10.1111/j.1365-4632.2008.03687.x.

5. Bragulla, H. H.; Homberger, D. G., Structure and functions of keratin proteins in simple, stratified, keratinized and cornified epithelia. *J Anat* **2009,** *214* (4), 516-59. DOI: 10.1111/j.1469-7580.2009.01066.x.

6. Meredith, P.; Riesz, J., Radiative relaxation quantum yields for synthetic eumelanin. *Photochem Photobiol* **2004,** *79* (2), 211-6.

7. Jenkins, G., Molecular mechanisms of skin ageing. *Mech Ageing Dev* **2002,** *123* (7), 801-10.

8. Merkel, J. R.; DiPaolo, B. R.; Hallock, G. G.; Rice, D. C., Type I and type III collagen content of healing wounds in fetal and adult rats. *Proc Soc Exp Biol Med* **1988,** *187* (4), 493-7.

9. Meigel, W. N.; Gay, S.; Weber, L., Dermal architecture and collagen type distribution. *Arch Dermatol Res* **1977,** *259* (1), 1-10.

10. Comper, W. D.; Laurent, T. C., Physiological function of connective tissue polysaccharides. *Physiol Rev* **1978,** *58* (1), 255-315.

11. Ikada, Y., Challenges in tissue engineering. *J R Soc Interface* **2006,** *3* (10), 589-601. DOI: 10.1098/rsif.2006.0124.

12. Mano, J. F.; Silva, G. A.; Azevedo, H. S.; Malafaya, P. B.; Sousa, R. A.; Silva, S. S.; Boesel, L. F.; Oliveira, J. M.; Santos, T. C.; Marques, A. P.; Neves, N. M.; Reis, R. L., Natural origin biodegradable systems in tissue engineering and regenerative medicine: present status and some moving trends. *J R Soc Interface* **2007,** *4* (17), 999-1030. DOI: 10.1098/rsif.2007.0220.

13. Mammadov, R.; Mammadov, B.; Guler, M.; Tekinay, A., Growth Factor Binding on Heparin Mimetic Peptide Nanofibers. *Biomacromolecules* **2012,** *13* (10), 3311-3319. DOI: 10.1021/bm3010897.

14. Mann, B. K.; Schmedlen, R. H.; West, J. L., Tethered-TGF-beta increases extracellular matrix production of vascular smooth muscle cells. *Biomaterials* **2001,** *22* (5), 439-44.

15. Tayalia, P.; Mooney, D. J., Controlled growth factor delivery for tissue engineering. *Adv Mater* **2009,** *21* (32-33), 3269-85. DOI: 10.1002/adma.200900241.

16. Gama, C. I.; Tully, S. E.; Sotogaku, N.; Clark, P. M.; Rawat, M.; Vaidehi, N.; Goddard, W. A.; Nishi, A.; Hsieh-Wilson, L. C., Sulfation patterns of glycosaminoglycans encode molecular recognition and activity. *Nat Chem Biol* **2006,** *2* (9), 467-73. DOI: 10.1038/nchembio810.

17. Pellegrini, L.; Burke, D. F.; von Delft, F.; Mulloy, B.; Blundell, T. L., Crystal structure of fibroblast growth factor receptor ectodomain bound to ligand and heparin. *Nature* **2000,** *407* (6807), 1029-34. DOI: 10.1038/35039551.

18. Liu, L. S.; Ng, C. K.; Thompson, A. Y.; Poser, J. W.; Spiro, R. C., Hyaluronate-heparin conjugate gels for the delivery of basic fibroblast growth factor (FGF-2). *J Biomed Mater Res* **2002,** *62* (1), 128-35. DOI: 10.1002/jbm.10238.

19. Lutolf, M.; Hubbell, J., Synthetic biomaterials as instructive extracellular microenvironments for morphogenesis in tissue engineering. *Nature Biotechnology* **2005,** *23* (1), 47-55. DOI: 10.1038/nbt1055.

20. Mecham, R. P., Overview of extracellular matrix. *Current protocols in cell biology / editorial board, Juan S. Bonifacino ... [et al.]* **2001,** *Chapter 10*, Unit 10.1-Unit 10.1.

21. Mouw, J. K.; Ou, G.; Weaver, V. M., Extracellular matrix assembly: a multiscale deconstruction. *Nat Rev Mol Cell Biol* **2014,** *15* (12), 771-85. DOI: 10.1038/nrm3902.

22. Iozzo, R. V.; Murdoch, A. D., Proteoglycans of the extracellular environment: clues from the gene and protein side offer novel perspectives in molecular diversity and function. *FASEB J* **1996,** *10* (5), 598-614.

23. Schaefer, L.; Schaefer, R. M., Proteoglycans: from structural compounds to signaling molecules. *Cell Tissue Res* **2010,** *339* (1), 237-46. DOI: 10.1007/s00441-009-0821-y.

24. Badylak, S. F., The extracellular matrix as a scaffold for tissue reconstruction. *Semin Cell Dev Biol* **2002,** *13* (5), 377-83.

25. Iozzo, R. V.; San Antonio, J. D., Heparan sulfate proteoglycans: heavy hitters in the angiogenesis arena. *J Clin Invest* **2001,** *108* (3), 349-55. DOI: 10.1172/JCI13738.

26. Carulli, D.; Laabs, T.; Geller, H. M.; Fawcett, J. W., Chondroitin sulfate proteoglycans in neural development and regeneration. *Curr Opin Neurobiol* **2005,** *15* (1), 116-20. DOI: 10.1016/j.conb.2005.01.014.

27. Sugahara, K.; Mikami, T.; Uyama, T.; Mizuguchi, S.; Nomura, K.; Kitagawa, H., Recent advances in the structural biology of chondroitin sulfate and dermatan sulfate. *Curr Opin Struct Biol* **2003,** *13* (5), 612-20.

28. Casu, B.; Guerrini, M.; Torri, G., Structural and conformational aspects of the anticoagulant and anti-thrombotic activity of heparin and dermatan sulfate. *Curr Pharm Des* **2004,** *10* (9), 939-49.

29. Lin, X., Functions of heparan sulfate proteoglycans in cell signaling during development. *Development* **2004,** *131* (24), 6009-21. DOI: 10.1242/dev.01522.

30. Murugan, R.; Ramakrishna, S., Design strategies of tissue engineering scaffolds with controlled fiber orientation. *Tissue Eng* **2007,** *13* (8), 1845-66. DOI: 10.1089/ten.2006.0078.

31. Berthiaume, F.; Maguire, T. J.; Yarmush, M. L., Tissue engineering and regenerative medicine: history, progress, and challenges. *Annu Rev Chem Biomol Eng* **2011,** *2*, 403-30. DOI: 10.1146/annurev-chembioeng-061010-114257.

32. Griffith, L. G.; Naughton, G., Tissue engineering--current challenges and expanding opportunities. *Science* **2002,** *295* (5557), 1009-14. DOI: 10.1126/science.1069210.

33. Hollister, S. J., Porous scaffold design for tissue engineering. *Nat Mater* **2005,** *4* (7), 518-24. DOI: 10.1038/nmat1421.

34. Place, E. S.; Evans, N. D.; Stevens, M. M., Complexity in biomaterials for tissue engineering. *Nat Mater* **2009,** *8* (6), 457-70. DOI: 10.1038/nmat2441.

35. Dvir, T.; Timko, B. P.; Kohane, D. S.; Langer, R., Nanotechnological strategies for engineering complex tissues. *Nat Nanotechnol* **2011,** *6* (1), 13-22. DOI: 10.1038/nnano.2010.246.

36. Brown, B. N.; Valentin, J. E.; Stewart-Akers, A. M.; McCabe, G. P.; Badylak, S. F., Macrophage phenotype and remodeling outcomes in response to biologic scaffolds with and without a cellular component. *Biomaterials* **2009,** *30* (8), 1482-91. DOI: 10.1016/j.biomaterials.2008.11.040.

37. Collins, M. N.; Birkinshaw, C., Hyaluronic acid based scaffolds for tissue engineering--a review. *Carbohydr Polym* **2013,** *92* (2), 1262-79. DOI: 10.1016/j.carbpol.2012.10.028.

38. Nair, L.; Laurencin, C., Biodegradable polymers as biomaterials. *Progress in Polymer Science* **2007,** *32* (8-9), 762-798. DOI: 10.1016/j.progpolymsci.2007.05.017.

39. Barnes, C. P.; Pemble, C. W.; Brand, D. D.; Simpson, D. G.; Bowlin, G. L., Cross-linking electrospun type II collagen tissue engineering scaffolds with carbodiimide in ethanol. *Tissue Eng* **2007,** *13* (7), 1593-605. DOI: 10.1089/ten.2006.0292.

40. Atala, A., Tissue engineering and regenerative medicine: concepts for clinical application. *Rejuvenation Res* **2004,** *7* (1), 15-31. DOI: 10.1089/154916804323105053.

41. Chen, G.; Ushida, T.; Tateishi, T., A biodegradable hybrid sponge nested with collagen microsponges. *J Biomed Mater Res* **2000,** *51* (2), 273-9.

42. Knight, C. G.; Morton, L. F.; Peachey, A. R.; Tuckwell, D. S.; Farndale, R. W.; Barnes, M. J., The collagen-binding A-domains of integrins alpha(1)beta(1) and alpha(2)beta(1) recognize the same specific amino acid sequence, GFOGER, in native (triple-helical) collagens. *J Biol Chem* **2000,** *275* (1), 35-40.

43. Konitsiotis, A. D.; Raynal, N.; Bihan, D.; Hohenester, E.; Farndale, R. W.; Leitinger, B., Characterization of high affinity binding motifs for the discoidin

domain receptor DDR2 in collagen. *J Biol Chem* **2008,** *283* (11), 6861-8. DOI: 10.1074/jbc.M709290200.

44. Pierschbacher, M. D.; Ruoslahti, E., Cell attachment activity of fibronectin can be duplicated by small synthetic fragments of the molecule. *Nature* **1984,** *309* (5963), 30-3.

45. Fiedler, L. R.; Schönherr, E.; Waddington, R.; Niland, S.; Seidler, D. G.; Aeschlimann, D.; Eble, J. A., Decorin regulates endothelial cell motility on collagen I through activation of insulin-like growth factor I receptor and modulation of alpha2beta1 integrin activity. *J Biol Chem* **2008,** *283* (25), 17406-15. DOI: 10.1074/jbc.M710025200.

46. Edmonds, M.; Group, E. a. A. A. D. F. U. S., Apligraf in the treatment of neuropathic diabetic foot ulcers. *Int J Low Extrem Wounds* **2009,** *8* (1), 11-8. DOI: 10.1177/1534734609331597.

47. Jean, J.; Lapointe, M.; Soucy, J.; Pouliot, R., Development of an in vitro psoriatic skin model by tissue engineering. *J Dermatol Sci* **2009,** *53* (1), 19-25. DOI: 10.1016/j.jdermsci.2008.07.009.

48. Régnier, M.; Staquet, M. J.; Schmitt, D.; Schmidt, R., Integration of Langerhans cells into a pigmented reconstructed human epidermis. *J Invest Dermatol* **1997,** *109* (4), 510-2.

49. L'Heureux, N.; Pâquet, S.; Labbé, R.; Germain, L.; Auger, F. A., A completely biological tissue-engineered human blood vessel. *FASEB J* **1998,** *12* (1), 47-56.

50. Grueterich, M.; Espana, E. M.; Tseng, S. C., Ex vivo expansion of limbal epithelial stem cells: amniotic membrane serving as a stem cell niche. *Surv Ophthalmol* **2003,** *48* (6), 631-46.

51. Harley, B. A.; Lynn, A. K.; Wissner-Gross, Z.; Bonfield, W.; Yannas, I. V.; Gibson, L. J., Design of a multiphase osteochondral scaffold. II. Fabrication of a mineralized collagen-glycosaminoglycan scaffold. *J Biomed Mater Res A* **2010,** *92* (3), 1066-77. DOI: 10.1002/jbm.a.32361.

52. Tedder, M. E.; Liao, J.; Weed, B.; Stabler, C.; Zhang, H.; Simionescu, A.; Simionescu, D. T., Stabilized collagen scaffolds for heart valve tissue engineering. *Tissue Eng Part A* **2009,** *15* (6), 1257-68. DOI: 10.1089/ten.tea.2008.0263.

53. Bouhout, S.; Perron, E.; Gauvin, R.; Bernard, G.; Ouellet, G.; Cattan, V.; Bolduc, S., In vitro reconstruction of an autologous, watertight, and resistant vesical equivalent. *Tissue Eng Part A* **2010,** *16* (5), 1539-48. DOI: 10.1089/ten.TEA.2009.0473.

54. Gingras, M.; Beaulieu, M. M.; Gagnon, V.; Durham, H. D.; Berthod, F., In vitro study of axonal migration and myelination of motor neurons in a three-dimensional tissue-engineered model. *Glia* **2008,** *56* (3), 354-64. DOI: 10.1002/glia.20617.

55. Boeriu, C. G.; Springer, J.; Kooy, F. K.; van den Broek, L. A. M.; Eggink, G., Production Methods for Hyaluronan. *International Journal of Carbohydrate Chemistry* **2013,** *2013*, 14. DOI: 10.1155/2013/624967.

56. Hascall, V., Hyaluronan, a common thread. *Glycoconjugate Journal* **2000,** *17* (7-9), 607-616. DOI: 10.1023/A:1011082728155.

57. Freymann, U.; Endres, M.; Neumann, K.; Scholman, H. J.; Morawietz, L.; Kaps, C., Expanded human meniscus-derived cells in 3-D polymer-hyaluronan scaffolds for meniscus repair. *Acta biomaterialia* **2012,** *8* (2), 677-85.

58. Tan, H.; Chu, C. R.; Payne, K. A.; Marra, K. G., Injectable in situ forming biodegradable chitosan-hyaluronic acid based hydrogels for cartilage tissue engineering. *Biomaterials* **2009,** *30* (13), 2499-506.

59. Toh, W.; Lim, T.; Kurisawa, M.; Spector, M., Modulation of mesenchymal stem cell chondrogenesis in a tunable hyaluronic acid hydrogel microenvironment. *Biomaterials* **2012,** *33* (15), 3835-3845. DOI: 10.1016/j.biomaterials.2012.01.065.

60. Park, J.; Shim, J.; Kang, K.; Yeom, J.; Jung, H.; Kim, J.; Lee, K.; Kim, T.; Kim, S.; Cho, D.; Hahn, S., Solid Free-Form Fabrication of Tissue-Engineering Scaffolds with a Poly(lactic-co-glycolic acid) Grafted Hyaluronic Acid Conjugate Encapsulating an Intact Bone Morphogenetic Protein-2/Poly(ethylene glycol) Complex. *Advanced Functional Materials* **2011,** *21* (15), 2906-2912. DOI: 10.1002/adfm.201100612.

61. Faga, A.; Nicoletti, G.; Brenta, F.; Scevola, S.; Abatangelo, G.; Brun, P., Hyaluronic acid three-dimensional scaffold for surgical revision of retracting scars: a human experimental study. *International Wound Journal* **2013,** *10* (3), 329-335. DOI: 10.1111/j.1742-481X.2012.00981.x.

62. Ananthanarayanan, B.; Kim, Y.; Kumar, S., Elucidating the mechanobiology of malignant brain tumors using a brain matrix-mimetic hyaluronic acid hydrogel platform. *Biomaterials* **2011,** *32* (31), 7913-23. DOI: 10.1016/j.biomaterials.2011.07.005.

63. Fagien, S.; Cassuto, D., Reconstituted injectable hyaluronic acid: expanded applications in facial aesthetics and additional thoughts on the mechanism of action in cosmetic medicine. *Plast Reconstr Surg* **2012,** *130* (1), 208-17. DOI: 10.1097/PRS.0b013e318254b3f6.

64. George, M.; Abraham, T. E., Polyionic hydrocolloids for the intestinal delivery of protein drugs: alginate and chitosan--a review. *J Control Release* **2006,** *114* (1), 1-14. DOI: 10.1016/j.jconrel.2006.04.017.

65. Stevens, M. M.; Qanadilo, H. F.; Langer, R.; Prasad Shastri, V., A rapid-curing alginate gel system: utility in periosteum-derived cartilage tissue engineering. *Biomaterials* **2004,** *25* (5), 887-94.

66. Hubbell, J., Bioactive biomaterials. *Current Opinion in Biotechnology* **1999,** *10* (2), 123-129. DOI: 10.1016/S0958-1669(99)80021-4.

67. Kuo, C. K.; Ma, P. X., Ionically crosslinked alginate hydrogels as scaffolds for tissue engineering: part 1. Structure, gelation rate and mechanical properties. *Biomaterials* **2001,** *22* (6), 511-21.

68. Boontheekul, T.; Kong, H. J.; Mooney, D. J., Controlling alginate gel degradation utilizing partial oxidation and bimodal molecular weight distribution. *Biomaterials* **2005,** *26* (15), 2455-65. DOI: 10.1016/j.biomaterials.2004.06.044.

69. Cole, S. M.; Garbe, J. E., Alginate hydrogel foam wound dressing. Google Patents: 1990.

70. Opara, E. C.; McQuilling, J. P.; Farney, A. C., Microencapsulation of pancreatic islets for use in a bioartificial pancreas. *Methods Mol Biol* **2013,** *1001*, 261-6. DOI: 10.1007/978-1-62703-363-3_21.

71. Smidsrød, O.; Skjåk-Braek, G., Alginate as immobilization matrix for cells. *Trends Biotechnol* **1990,** *8* (3), 71-8.

72. Rao, S.; Sharma, C., Use of chitosan as a biomaterial: Studies on its safety and hemostatic potential. *Journal of Biomedical Materials Research* **1997,** *34* (1), 21-28. DOI: 10.1002/(SICI)1097-4636(199701)34:1<21::AID-JBM4>3.0.CO;2-P.

73. Croisier, F.; Jerome, C., Chitosan-based biomaterials for tissue engineering. *European Polymer Journal* **2013,** *49* (4), 780-792. DOI: 10.1016/j.eurpolymj.2012.12.009.

74. Azad, A.; Sermsintham, N.; Chandrkrachang, S.; Stevens, W., Chitosan membrane as a wound-healing dressing: Characterization and clinical application. *Journal of Biomedical Materials Research Part B-Applied Biomaterials* **2004,** *69B* (2), 216-222. DOI: 10.1002/jbm.b.30000.

75. Suh, J.; Matthew, H., Application of chitosan-based polysaccharide biomaterials in cartilage tissue engineering: a review. *Biomaterials* **2000,** *21* (24), 2589-2598.

76. Ao, Q.; Fung, C.; Tsui, A.; Cai, S.; Zuo, H.; Chan, Y.; Shum, D., The regeneration of transected sciatic nerves of adult rats using chitosan nerve conduits seeded with bone marrow stromal cell-derived Schwann cells. *Biomaterials* **2011,** *32* (3), 787-796. DOI: 10.1016/j.biomaterials.2010.09.046.

77. Pashuck, E. T.; Stevens, M. M., Designing regenerative biomaterial therapies for the clinic. *Sci Transl Med* **2012,** *4* (160), 160sr4. DOI: 10.1126/scitranslmed.3002717.

78. Calonder, C.; Matthew, H. W.; Van Tassel, P. R., Adsorbed layers of oriented fibronectin: a strategy to control cell-surface interactions. *J Biomed Mater Res A* **2005,** *75* (2), 316-23. DOI: 10.1002/jbm.a.30417.

79. Perka, C.; Spitzer, R. S.; Lindenhayn, K.; Sittinger, M.; Schultz, O., Matrix-mixed culture: new methodology for chondrocyte culture and preparation of cartilage transplants. *J Biomed Mater Res* **2000,** *49* (3), 305-11.

80. Wang, Y.; Kim, U. J.; Blasioli, D. J.; Kim, H. J.; Kaplan, D. L., In vitro cartilage tissue engineering with 3D porous aqueous-derived silk scaffolds and

mesenchymal stem cells. *Biomaterials* **2005,** *26* (34), 7082-94. DOI: 10.1016/j.biomaterials.2005.05.022.

81. Balgude, A. P.; Yu, X.; Szymanski, A.; Bellamkonda, R. V., Agarose gel stiffness determines rate of DRG neurite extension in 3D cultures. *Biomaterials* **2001,** *22* (10), 1077-84.

82. Lévesque, S. G.; Lim, R. M.; Shoichet, M. S., Macroporous interconnected dextran scaffolds of controlled porosity for tissue-engineering applications. *Biomaterials* **2005,** *26* (35), 7436-46. DOI: 10.1016/j.biomaterials.2005.05.054.

83. Magnusson, J.; Saeed, A.; Fernandez-Trillo, F.; Alexander, C., Synthetic polymers for biopharmaceutical delivery. *Polymer Chemistry* **2011,** *2* (1), 48-59. DOI: 10.1039/c0py00210k.

84. Oh, S.; Kang, S.; Kim, E.; Cho, S.; Lee, J., Fabrication and characterization of hydrophilic poly(lactic-co-glycolic acid)/poly(vinyl alcohol) blend cell scaffolds by melt-molding particulate-leaching method. *Biomaterials* **2003,** *24* (22), 4011-4021. DOI: 10.1016/S0142-9612(03)00284-9.

85. Ma, P., Scaffolds for tissue fabrication. *Materials Today* **2004,** *7* (5), 30-40. DOI: 10.1016/S1369-7021(04)00233-0.

86. O'Brien, F., Biomaterials & scaffolds for tissue engineering. *Materials Today* **2011,** *14* (3), 88-95. DOI: 10.1016/S1369-7021(11)70058-X.

87. Guo, B.; Ma, P., Synthetic biodegradable functional polymers for tissue engineering: a brief review. *Science China-Chemistry* **2014,** *57* (4), 490-500. DOI: 10.1007/s11426-014-5086-y.

88. Jain, J.; Chitkara, D.; Kumar, N., Polyanhydrides as localized drug delivery carrier: an update. *Expert Opinion on Drug Delivery* **2008,** *5* (8), 889-907. DOI: 10.1517/17425247.5.8.889|10.1517/17425240802305270.

89. Santerre, J.; Woodhouse, K.; Laroche, G.; Labow, R., Understanding the biodegradation of polyurethanes: From classical implants to tissue engineering materials. *Biomaterials* **2005,** *26* (35), 7457-7470. DOI: 10.1016/j.biomaterials.2005.05.079.

90. Sreejalekshmi, K.; Nair, P., Biomimeticity in tissue engineering scaffolds through synthetic peptide modifications-Altering chemistry for enhanced biological response. *Journal of Biomedical Materials Research Part a* **2011,** *96A* (2), 477-491. DOI: 10.1002/jbm.a.32980.

91. Lee, K.; Mooney, D., Hydrogels for tissue engineering. *Chemical Reviews* **2001,** *101* (7), 1869-1879. DOI: 10.1021/cr000108x.

92. Ovsianikov, A.; Deiwick, A.; Van Vlierberghe, S.; Dubruel, P.; Moller, L.; Drager, G.; Chichkov, B., Laser Fabrication of Three-Dimensional CAD Scaffolds from Photosensitive Gelatin for Applications in Tissue Engineering. *Biomacromolecules* **2011,** *12* (4), 851-858. DOI: 10.1021/bm1015305.

93. Cruise, G.; Hegre, O.; Lamberti, F.; Hager, S.; Hill, R.; Scharp, D.; Hubbell, J., In vitro and in vivo performance of porcine islets encapsulated in interfacially photopolymerized poly(ethylene glycol) diacrylate membranes. *Cell Transplantation* **1999,** *8* (3), 293-306.

94. Bryant, S.; Anseth, K., The effects of scaffold thickness on tissue engineered cartilage in photocrosslinked poly(ethylene oxide) hydrogels. *Biomaterials* **2001,** *22* (6), 619-626. DOI: 10.1016/S0142-9612(00)00225-8.

95. Burdick, J.; Anseth, K., Photoencapsulation of osteoblasts in injectable RGD-modified PEG hydrogels for bone tissue engineering. *Biomaterials* **2002,** *23* (22), 4315-4323. DOI: 10.1016/S0142-9612(02)00176-X.

96. Bohl, K.; West, J., Nitric oxide-generating polymers reduce platelet adhesion and smooth muscle cell proliferation. *Biomaterials* **2000,** *21* (22), 2273-2278. DOI: 10.1016/S0142-9612(00)00153-8.

97. Monnard, P.; Deamer, D., Membrane self-assembly processes: Steps toward the first cellular life. *Anatomical Record* **2002,** *268* (3), 196-207. DOI: 10.1002/ar.10154.

98. Stupp, S., Functional supramolecular polymers. *Abstracts of Papers of the American Chemical Society* **2012,** *243*.

99. Hartgerink, J.; Beniash, E.; Stupp, S., Peptide-amphiphile nanofibers: A versatile scaffold for the preparation of self-assembling materials. *Proceedings of the National Academy of Sciences of the United States of America* **2002,** *99* (8), 5133-5138. DOI: 10.1073/pnas.072699999.

100. Niece, K. L.; Hartgerink, J. D.; Donners, J. J.; Stupp, S. I., Self-assembly combining two bioactive peptide-amphiphile molecules into nanofibers by electrostatic attraction. *J Am Chem Soc* **2003,** *125* (24), 7146-7. DOI: 10.1021/ja028215r.

101. Rudra, J.; Sun, T.; Bird, K.; Daniels, M.; Gasiorowski, J.; Chong, A.; Collier, J., Modulating Adaptive Immune Responses to Peptide Self-Assemblies. *Acs Nano* **2012,** *6* (2), 1557-1564. DOI: 10.1021/nn204530r.

102. Lin, Y.; Luo, C.; Hu, Y.; Yeh, M.; Hsueh, Y.; Chang, M.; Tsai, D.; Wang, J.; Tang, M.; Wei, E.; Springer, M.; Hsieh, P., Instructive Nanofiber Scaffolds with VEGF Create a Microenvironment for Arteriogenesis and Cardiac Repair. *Science Translational Medicine* **2012,** *4* (146). DOI: 10.1126/scitranslmed.3003841.

103. Mammadov, B.; Mammadov, R.; Guler, M.; Tekinay, A., Cooperative effect of heparan sulfate and laminin mimetic peptide nanofibers on the promotion of neurite

outgrowth. *Acta Biomaterialia* **2012,** *8* (6), 2077-2086. DOI: 10.1016/j.actbio.2012.02.006.

104. Ustun, S.; Tombuloglu, A.; Kilinc, M.; Guler, M.; Tekinay, A., Growth and Differentiation of Prechondrogenic Cells on Bioactive Self-Assembled Peptide Nanofibers. *Biomacromolecules* **2013,** *14* (1), 17-26. DOI: 10.1021/bm301538k.

105. Ceylan, H.; Kocabey, S.; Gulsuner, H.; Balcik, O.; Guler, M.; Tekinay, A., Bone-Like Mineral Nucleating Peptide Nanofibers Induce Differentiation of Human Mesenchymal Stem Cells into Mature Osteoblasts. *Biomacromolecules* **2014,** *15* (7), 2407-2418. DOI: 10.1021/bm500248r.

106. Sever, M.; Mammadov, B.; Guler, M.; Tekinay, A., Tenascin-C Mimetic Peptide Nanofibers Direct Stem Cell Differentiation to Osteogenic Lineage. *Biomacromolecules* **2014,** *15* (12), 4480-4487. DOI: 10.1021/bm501271x.

107. Bulut, S.; Erkal, T.; Toksoz, S.; Tekinay, A.; Tekinay, T.; Guler, M., Slow Release and Delivery of Antisense Oligonucleotide Drug by Self-Assembled Peptide Amphiphile Nanofibers. *Biomacromolecules* **2011,** *12* (8), 3007-3014. DOI: 10.1021/bm200641e.

108. Matson, J. B.; Newcomb, C. J.; Bitton, R.; Stupp, S. I., Nanostructure-templated control of drug release from peptide amphiphile nanofiber gels. *Soft Matter* **2012,** *8* (13), 3586-3595.

109. Weis, S. M.; Cheresh, D. A., Tumor angiogenesis: molecular pathways and therapeutic targets. *Nat Med* **2011,** *17* (11), 1359-70. DOI: 10.1038/nm.2537.

110. Logsdon, E. A.; Finley, S. D.; Popel, A. S.; Mac Gabhann, F., A systems biology view of blood vessel growth and remodelling. *J Cell Mol Med* **2014,** *18* (8), 1491-508. DOI: 10.1111/jcmm.12164.

111. Lang, G. E., Diabetic macular edema. *Ophthalmologica* **2012,** *227 Suppl 1*, 21-9. DOI: 10.1159/000337156.

112. Brem, H.; Tomic-Canic, M., Cellular and molecular basis of wound healing in diabetes. *J Clin Invest* **2007,** *117* (5), 1219-22. DOI: 10.1172/JCI32169.

113. Bruls, W. A.; Slaper, H.; van der Leun, J. C.; Berrens, L., Transmission of human epidermis and stratum corneum as a function of thickness in the ultraviolet and visible wavelengths. *Photochem Photobiol* **1984,** *40* (4), 485-94.

114. Li, J.; Post, M.; Volk, R.; Gao, Y.; Li, M.; Metais, C.; Sato, K.; Tsai, J.; Aird, W.; Rosenberg, R. D.; Hampton, T. G.; Sellke, F.; Carmeliet, P.; Simons, M., PR39, a peptide regulator of angiogenesis. *Nat Med* **2000,** *6* (1), 49-55. DOI: 10.1038/71527.

115. Hamada, Y.; Egusa, H.; Kaneda, Y.; Hirata, I.; Kawaguchi, N.; Hirao, T.; Matsumoto, T.; Yao, M.; Daito, K.; Suzuki, M.; Yatani, H.; Daito, M.; Okazaki, M.; Matsuura, N., Synthetic osteopontin-derived peptide SVVYGLR can induce neovascularization in artificial bone marrow scaffold biomaterials. *Dent Mater J* **2007,** *26* (4), 487-92.

116. Arap, W.; Pasqualini, R.; Ruoslahti, E., Cancer treatment by targeted drug delivery to tumor vasculature in a mouse model. *Science* **1998,** *279* (5349), 377-80.

117. Reinke, J. M.; Sorg, H., Wound repair and regeneration. *Eur Surg Res* **2012,** *49* (1), 35-43. DOI: 10.1159/000339613.

118. Uzunalli, G.; Mammadov, R.; Yesildal, F.; Alhan, D.; Ozturk, S.; Ozgurtas, T.; Guler, M. O.; Tekinay, A. B., Angiogenic Heparin-Mimetic Peptide Nanofiber Gel Improves Regenerative Healing of Acute Wounds. *ACS Biomaterials Science & Engineering* **2016**. DOI: 10.1021/acsbiomaterials.6b00165.

119. MacNeil, S., Biomaterials for tissue engineering of skin. *Materials Today* **2008,** *11* (5), 26-35. DOI: 10.1016/S1369-7021(08)70087-7.

120. Yildirimer, L.; Thanh, N. T.; Seifalian, A. M., Skin regeneration scaffolds: a multimodal bottom-up approach. *Trends Biotechnol* **2012,** *30* (12), 638-48. DOI: 10.1016/j.tibtech.2012.08.004.

121. Gurtner, G. C.; Werner, S.; Barrandon, Y.; Longaker, M. T., Wound repair and regeneration. *Nature* **2008,** *453* (7193), 314-21. DOI: 10.1038/nature07039.

122. Singer, A. J.; Clark, R. A., Cutaneous wound healing. *N Engl J Med* **1999,** *341* (10), 738-46. DOI: 10.1056/NEJM199909023411006.

123. Martin, P., Wound healing - Aiming for perfect skin regeneration. *Science* **1997,** *276* (5309), 75-81. DOI: 10.1126/science.276.5309.75.

124. Boateng, J.; Matthews, K.; Stevens, H.; Eccleston, G., Wound healing dressings and drug delivery systems: A review. *Journal of Pharmaceutical Sciences* **2008,** *97* (8), 2892-2923. DOI: 10.1002/jps.21210.

125. Priya, S.; Jungvid, H.; Kumar, A., Skin tissue engineering for tissue repair and regeneration. *Tissue Engineering Part B-Reviews* **2008,** *14* (1), 105-118. DOI: 10.1089/teb.2007.0318.

126. Worthington, P.; Pochan, D. J.; Langhans, S. A., Peptide Hydrogels - Versatile Matrices for 3D Cell Culture in Cancer Medicine. *Front Oncol* **2015,** *5*, 92. DOI: 10.3389/fonc.2015.00092.

127. Kokkoli, E.; Mardilovich, A.; Wedekind, A.; Rexeisen, E.; Garg, A.; Craig, J., Self-assembly and applications of biomimetic and bioactive peptide-amphiphiles. *Soft Matter* **2006,** *2* (12), 1015-1024. DOI: 10.1039/b608929a.

128. Yokoi, H.; Kinoshita, T.; Zhang, S., Dynamic reassembly of peptide RADA16 nanofiber scaffold. *Proceedings of the National Academy of Sciences of the United States of America* **2005,** *102* (24), 8414-8419. DOI: 10.1073/pnas.0407843102.

129. Luo, Z.; Yue, Y.; Zhang, Y.; Yuan, X.; Gong, J.; Wang, L.; He, B.; Liu, Z.; Sun, Y.; Liu, J.; Hu, M.; Zheng, J., Designer D-form self-assembling peptide nanofiber scaffolds for 3-dimensional cell cultures. *Biomaterials* **2013,** *34* (21), 4902-13. DOI: 10.1016/j.biomaterials.2013.03.081.

130. Luo, Z.; Wang, S.; Zhang, S., Fabrication of self-assembling D-form peptide nanofiber scaffold d-EAK16 for rapid hemostasis. *Biomaterials* **2011,** *32* (8), 2013-20. DOI: 10.1016/j.biomaterials.2010.11.049.

131. Yasa, I. C.; Gunduz, N.; Kilinc, M.; Guler, M. O.; Tekinay, A. B., Basal Lamina Mimetic Nanofibrous Peptide Networks for Skeletal Myogenesis. *Sci Rep* **2015,** *5*, 16460. DOI: 10.1038/srep16460.

132. Kao, B.; Kadomatsu, K.; Hosaka, Y., Construction of synthetic dermis and skin based on a self-assembled peptide hydrogel scaffold. *Tissue Eng Part A* **2009,** *15* (9), 2385-96. DOI: 10.1089/ten.tea.2008.0362.

133. Seow, W.; Salgado, G.; Lane, E.; Hauser, C., Transparent crosslinked ultrashort peptide hydrogel dressing with high shape-fidelity accelerates healing of full-thickness excision wounds. *Scientific Reports* **2016,** *6*. DOI: 10.1038/srep32670.

134. Hunt, N. C.; Grover, L. M., Cell encapsulation using biopolymer gels for regenerative medicine. *Biotechnol Lett* **2010,** *32* (6), 733-42. DOI: 10.1007/s10529-010-0221-0.

135. Kim, J. K.; Kim, H. J.; Chung, J. Y.; Lee, J. H.; Young, S. B.; Kim, Y. H., Natural and synthetic biomaterials for controlled drug delivery. *Arch Pharm Res* **2014,** *37* (1), 60-8. DOI: 10.1007/s12272-013-0280-6.

136. Gelain, F.; Unsworth, L. D.; Zhang, S., Slow and sustained release of active cytokines from self-assembling peptide scaffolds. *J Control Release* **2010,** *145* (3), 231-9. DOI: 10.1016/j.jconrel.2010.04.026.

137. Kopesky, P. W.; Byun, S.; Vanderploeg, E. J.; Kisiday, J. D.; Frisbie, D. D.; Grodzinsky, A. J., Sustained delivery of bioactive TGF-β1 from self-assembling peptide hydrogels induces chondrogenesis of encapsulated bone marrow stromal cells. *J Biomed Mater Res A* **2014,** *102* (5), 1275-85. DOI: 10.1002/jbm.a.34789.

138. Schneider, A.; Garlick, J. A.; Egles, C., Self-assembling peptide nanofiber scaffolds accelerate wound healing. *PLoS One* **2008,** *3* (1), e1410. DOI: 10.1371/journal.pone.0001410.

139. Koria, P.; Yagi, H.; Kitagawa, Y.; Megeed, Z.; Nahmias, Y.; Sheridan, R.; Yarmush, M. L., Self-assembling elastin-like peptides growth factor chimeric nanoparticles for the treatment of chronic wounds. *Proc Natl Acad Sci U S A* **2011,** *108* (3), 1034-9. DOI: 10.1073/pnas.1009881108.

140. Rajangam, K.; Behanna, H.; Hui, M.; Han, X.; Hulvat, J.; Lomasney, J.; Stupp, S., Heparin binding nanostructures to promote growth of blood vessels. *Nano Letters* **2006,** *6* (9), 2086-2090. DOI: 10.1021/nl0613555.

141. Hosseinkhani, H.; Hosseinkhani, M.; Khademhosseini, A.; Kobayashi, H.; Tabata, Y., Enhanced angiogenesis through controlled release of basic fibroblast growth factor from peptide amphiphile for tissue regeneration. *Biomaterials* **2006,** *27* (34), 5836-5844. DOI: 10.1016/j.biomaterials.2006.08.003.

142. Mammadov, R.; Mammadov, B.; Toksoz, S.; Aydin, B.; Yagci, R.; Tekinay, A.; Guler, M., Heparin Mimetic Peptide Nanofibers Promote Angiogenesis. *Biomacromolecules* **2011,** *12* (10), 3508-3519. DOI: 10.1021/bm200957s.

143. Senturk, B.; Mercan, S.; Delibasi, T.; Guler, M.; Tekinay, A., Angiogenic Peptide Nanofibers Improve Wound Healing in STZ-Induced Diabetic Rats. *Acs Biomaterials Science & Engineering* **2016,** *2* (7), 1180-1189. DOI: 10.1021/acsbiomaterials.6b00238.

144. Yergoz, F.; Hastar, N.; Cimenci, C. E.; Ozkan, A. D.; Tekinay, T.; Guler, M. O.; Tekinay, A. B., Heparin mimetic peptide nanofiber gel promotes regeneration of full thickness burn injury. *Biomaterials* **2017,** *134*, 117-127. DOI: 10.1016/j.biomaterials.2017.04.040.

145. Rowan, M. P.; Cancio, L. C.; Elster, E. A.; Burmeister, D. M.; Rose, L. F.; Natesan, S.; Chan, R. K.; Christy, R. J.; Chung, K. K., Burn wound healing and treatment: review and advancements. *Crit Care* **2015,** *19*, 243. DOI: 10.1186/s13054-015-0961-2.

146. Madaghiele, M.; Demitri, C.; Sannino, A.; Ambrosio, L., Polymeric hydrogels for burn wound care: Advanced skin wound dressings and regenerative templates. *Burns Trauma* **2014,** *2* (4), 153-61. DOI: 10.4103/2321-3868.143616.

147. Salibian, A. A.; Rosario, A. T.; Severo, L. e. A.; Nguyen, L.; Banyard, D. A.; Toranto, J. D.; Evans, G. R.; Widgerow, A. D., Current concepts on burn wound conversion-A review of recent advances in understanding the secondary progressions of burns. *Burns* **2016,** *42* (5), 1025-35. DOI: 10.1016/j.burns.2015.11.007.

148. Singh, V.; Devgan, L.; Bhat, S.; Milner, S. M., The pathogenesis of burn wound conversion. *Ann Plast Surg* **2007,** *59* (1), 109-15. DOI: 10.1097/01.sap.0000252065.90759.e6.

149. Schmauss, D.; Rezaeian, F.; Finck, T.; Machens, H. G.; Wettstein, R.; Harder, Y., Treatment of secondary burn wound progression in contact burns-a systematic review of experimental approaches. *J Burn Care Res* **2015,** *36* (3), e176-89. DOI: 10.1097/BCR.0000000000000131.

150. Farina, J. A.; Rosique, M. J.; Rosique, R. G., Curbing inflammation in burn patients. *Int J Inflam* **2013,** *2013*, 715645. DOI: 10.1155/2013/715645.

151. Shakespeare, P., Burn wound healing and skin substitutes. *Burns* **2001,** *27* (5), 517-22.

152. Rubert Pérez, C. M.; Stephanopoulos, N.; Sur, S.; Lee, S. S.; Newcomb, C.; Stupp, S. I., The powerful functions of peptide-based bioactive matrices for regenerative medicine. *Ann Biomed Eng* **2015,** *43* (3), 501-14. DOI: 10.1007/s10439-014-1166-6.

153. Loo, Y.; Goktas, M.; Tekinay, A. B.; Guler, M. O.; Hauser, C. A.; Mitraki, A., Self-Assembled Proteins and Peptides as Scaffolds for Tissue Regeneration. *Adv Healthc Mater* **2015,** *4* (16), 2557-86. DOI: 10.1002/adhm.201500402.

154. Rajangam, K.; Behanna, H. A.; Hui, M. J.; Han, X.; Hulvat, J. F.; Lomasney, J. W.; Stupp, S. I., Heparin binding nanostructures to promote growth of blood vessels. *Nano Lett* **2006,** *6* (9), 2086-90. DOI: 10.1021/nl0613555.

155. Loo, Y.; Wong, Y. C.; Cai, E. Z.; Ang, C. H.; Raju, A.; Lakshmanan, A.; Koh, A. G.; Zhou, H. J.; Lim, T. C.; Moochhala, S. M.; Hauser, C. A., Ultrashort peptide nanofibrous hydrogels for the acceleration of healing of burn wounds. *Biomaterials* **2014,** *35* (17), 4805-14. DOI: 10.1016/j.biomaterials.2014.02.047.

156. Meng, H.; Chen, L.; Ye, Z.; Wang, S.; Zhao, X., The effect of a self-assembling peptide nanofiber scaffold (peptide) when used as a wound dressing for the treatment of deep second degree burns in rats. *J Biomed Mater Res B Appl Biomater* **2009,** *89* (2), 379-91. DOI: 10.1002/jbm.b.31226.

157. Chomczynski, P., A reagent for the single-step simultaneous isolation of RNA, DNA and proteins from cell and tissue samples. *Biotechniques* **1993,** *15* (3), 532-4, 536-7.

158. Hummon, A. B.; Lim, S. R.; Difilippantonio, M. J.; Ried, T., Isolation and solubilization of proteins after TRIzol extraction of RNA and DNA from patient material following prolonged storage. *Biotechniques* **2007,** *42* (4), 467-70, 472.

159. Sun, G.; Shen, Y. I.; Ho, C. C.; Kusuma, S.; Gerecht, S., Functional groups affect physical and biological properties of dextran-based hydrogels. *J Biomed Mater Res A* **2010,** *93* (3), 1080-90. DOI: 10.1002/jbm.a.32604.

160. Miller, M. C.; Nanchahal, J., Advances in the modulation of cutaneous wound healing and scarring. *BioDrugs : clinical immunotherapeutics, biopharmaceuticals and gene therapy* **2005,** *19* (6), 363-81.

161. Jewo, P. I.; Fadeyibi, I. O., Progress in burns research: a review of advances in burn pathophysiology. *Ann Burns Fire Disasters* **2015,** *28* (2), 105-15.

162. Olczyk, P.; Mencner, Ł.; Komosinska-Vassev, K., Diverse Roles of Heparan Sulfate and Heparin in Wound Repair. *Biomed Res Int* **2015,** *2015*, 549417. DOI: 10.1155/2015/549417.

163. Paluck, S. J.; Nguyen, T. H.; Maynard, H. D., Heparin-Mimicking Polymers: Synthesis and Biological Applications. *Biomacromolecules* **2016**. DOI: 10.1021/acs.biomac.6b01147.

164. Sun, G.; Zhang, X.; Shen, Y. I.; Sebastian, R.; Dickinson, L. E.; Fox-Talbot, K.; Reinblatt, M.; Steenbergen, C.; Harmon, J. W.; Gerecht, S., Dextran hydrogel scaffolds enhance angiogenic responses and promote complete skin regeneration during burn wound healing. *Proc Natl Acad Sci U S A* **2011,** *108* (52), 20976-81. DOI: 10.1073/pnas.1115973108.

165. Arslan, E.; Guler, M. O.; Tekinay, A. B., Glycosaminoglycan-Mimetic Signals Direct the Osteo/Chondrogenic Differentiation of Mesenchymal Stem Cells in a

Three-Dimensional Peptide Nanofiber Extracellular Matrix Mimetic Environment. *Biomacromolecules* **2016,** *17* (4), 1280-91. DOI: 10.1021/acs.biomac.5b01637.

166. Senturk, B.; Cubuk, M. O.; Ozmen, M. C.; Aydin, B.; Guler, M. O.; Tekinay, A. B., Inhibition of VEGF mediated corneal neovascularization by anti-angiogenic peptide nanofibers. *Biomaterials* **2016,** *107*, 124-32. DOI: 10.1016/j.biomaterials.2016.08.045.

167. Uzunalli, G.; Tumtas, Y.; Delibasi, T.; Yasa, O.; Mercan, S.; Guler, M. O.; Tekinay, A. B., Improving pancreatic islet in vitro functionality and transplantation efficiency by using heparin mimetic peptide nanofiber gels. *Acta Biomater* **2015,** *22*, 8-18. DOI: 10.1016/j.actbio.2015.04.032.

168. Penn, J. W.; Grobbelaar, A. O.; Rolfe, K. J., The role of the TGF-β family in wound healing, burns and scarring: a review. *Int J Burns Trauma* **2012,** *2* (1), 18-28.

169. Castleberry, S. A.; Golberg, A.; Sharkh, M. A.; Khan, S.; Almquist, B. D.; Austen, W. G.; Yarmush, M. L.; Hammond, P. T., Nanolayered siRNA delivery platforms for local silencing of CTGF reduce cutaneous scar contraction in third-degree burns. *Biomaterials* **2016,** *95*, 22-34. DOI: 10.1016/j.biomaterials.2016.04.007.

APPENDIX

Table 2. Table of copyright permission of references that are used in the thesis.

Reference Number	Supplier	License Number
6	Wolters Kluwer Health, Inc.	4082790248695
19	Nature Publishing Group	4066091256246
34	Nature Publishing Group	4066100885310

143	RightsLink / Elsevier	4104230437305